Investigating the effect of internal fixation stiffness on metaphyseal fracture healing in a mouse model

MASTER'S THESIS

Lidia Koval
Student ID: 8452466

Principal Supervisor: Dr Roland Steck
Associate Supervisors: Dr Devakara Epari
Prof Michael Schuetz

Institute of Health and Biomedical Innovation
Queensland University of Technology
60 Musk Ave
Kelvin Grove, QLD 4059
Australia

Email: lidiakoval82@gmail.com

TABLE OF CONTENTS

TITLE 4
ABSTRACT 5
SUPERVISORS AND THEIR CREDENTIALS 7
LIST OF TABLES 8
LIST OF FIGURES 8
LIST OF ABBREVIATIONS 10
STATEMENT OF AUTHORSHIP 12
ACKNOWLEDGEMENTS 13
1. INTRODUCTION 14
2. LONG BONES 14
2.1. Basic anatomy and organisation 14
2.2. Cortical and cancellous bone 15
2.3. Regions of the bone 17
2.4. Periosteum and endosteum 18
2.5. Blood supply 20
3. FRACTURE HEALING 23
3.1. Stages of healing 23
4. METAPHYSEAL FRACTURES 28
4.1. Epidemiology 28
4.2. Metaphyseal fracture healing 31
4.3. Principles of treatment of metaphyseal fractures 33
4.4. Stiff vs flexible fixation 36
5. ANIMAL MODELS OF FRACTURE HEALING AND MOUSEFIX® 39
5.1. Animal models of fracture healing 39
5.2. MouseFix® development 40
5.3. Use of MouseFix® in medical research 42
6. HYPOTHESES 44
6.1. Knowledge gaps 44
6.2. Objectives and Hypotheses 45
7. MATERIALS AND METHODS 46
7.3. Mechanical testing 52
7.4. MicroCT analysis of callus formation 57
7.5. Histologic and histomorphometric analysis 59

7.6. Statistical evaluation....60
8. RESULTS....61
8.1. Gross observation....61
8.2. Mechanical testing....62
8.3. MicroCT....67
8.4. Histologic and histomorphometric analysis....71
9. DISCUSSION....77
REFERENCES....89
10. APPENDICES....96

TITLE

Investigating the effect of internal fixation on metaphyseal fracture healing in a mouse model

ABSTRACT

Although fractures of the metaphysis, the transition zone between the bone shaft and the bone ends near the joints, are very common in clinical practice, and a detailed understanding of the healing of these fractures is currently lacking, there have been only a few experimental studies investigating their healing mechanism. So far, there is some evidence that rigidly stabilised fractures heal primarily through intramembranous ossification, whereas flexibly fixed fractures heal mainly through endochondral ossification, similar to diaphyseal fractures. In this study, a novel locking plate system, MouseFix®, was used to examine the healing of distal femur fractures in mice, aiming to shed light on the relationship between different fixation stiffnesses and different bone healing mechanisms in the trabecular bone of the metaphysis.

An osteotomy was performed in the distal femur in outbred albino mice after stabilization of the bone with locking mini-plates of one of three stiffnesses: 100% stiff (rigid), 65% stiff and 45% stiff. After sacrifice at 14 days and 28 days, representing an early and a late stage of healing, respectively, the bones were analysed radiologically, biomechanically and histologically.

There was no difference in callus volume between the groups at both healing stages, regardless of fixation type. Similarly, while bones stabilized with the 65% stiff implants appeared to have the lowest bending stiffness in the early stage and the highest bending stiffness in the late stage of healing, these differences between groups were not statistically significant. A limited histological analysis demonstrated cartilage production in both groups, indicating a combination of endochondral and

intramembranous ossification in the healing of metaphyseal fractures in mice, regardless of fixation stiffness.

Several challenges encountered in these experiments prevented a conclusive answer on the effect of fixation stiffness on metaphyseal bone healing mechanisms in mice. Thereby, this study highlighted some of the limitations in attempting to reproducibly stabilize metaphyseal osteotomies in mice femora. However, the lessons we learned from our experience with this model in this project, will help us and other researchers who contemplate the use of the MouseFix® system for studying metaphyseal bone healing, to optimize the experimental design of future studies.

SUPERVISORS AND THEIR CREDENTIALS

Dr Roland Stec kDr sc techn (ETH Zurich) – level 2 accredited

Dr Devakara Epari Dr.-Ing (Technical University of Berlin) – level 2 accredited

Prof Michael Schuetz FRACS, FAOrthA, Dr. med. (RWTH Aachen) Dr. med. habil (HU Berlin) – level 2 accredited

LIST OF TABLES

Table 1. Summary of studies, investigating healing of metaphyseal bone

Table 2. Flowchart summary of Materials and Methods

Table 3. Change in %Extrinsic Stiffness (%EI) at 14 day time point

Table 4.Change in %Extrinsic Stiffness (%EI) at 28-day time point

Table 5. Change in %Extrinsic Stiffness between two time points

Table 6. Callus Volume (V_{call}) at 14-day time point

Table 7. Callus Volume (V_{call}) at 28-day time point

Table 8. Mean callus volume (V_{call}) at 14-day and at 28-day time points in all groups

Table 9. Counts of cartilage in callus

Table 10. Results flowchart

LIST OF FIGURES

Fig. 1.Organisation of cortical and cancellous bone

Fig. 2. Classification of bone regions on the example of a femur

Fig. 3.Periosteum and endosteum

Fig. 4. Blood supply to the cortical bone

Fig. 5. Stages of bone healing

Fig. 6. Stage I: Inflammation

Fig. 7.Stage II: Proliferation

Fig. 8.Stage III: Consolidation

Fig. 9.Stage IV: Remodelling

Fig. 10.Endochondral ossification with callus formation

Fig. 11. Intramembranous ossification with direct ossification across the fracture gap

Fig. 12. Volar Locking Plate (VLP) applied to the distal radius

Fig. 13. MouseFix® plating system for metaphyseal fractures

Fig. 14.Two configurations of the MouseFix® plate: a) rigid b) flexible

Fig. 15.a) Self-tapping cortical locking screw and b) Drill guide

Fig. 16. Surgical approach: preparation of the femur

Fig. 17. Rigid MouseFix®plate, applied to the metaphysis of distal femur

Fig.18.Creation of the transverse osteotomy with a Gigli saw

Fig. 19. Sacrifice by CO2 asphyxiation

Fig. 20.Three-point flexural stiffness test

Fig. 21.Three-point bending test of a mouse femur

Fig. 22. Measuring the distance between the supports and the top point load

Fig. 23. The load-deformation curve

Fig. 24. %Extrinsic Stiffness (%EI) at 14-day time point

Fig. 25. %Extrinsic Stiffness (%EI) at 28-day time point

Fig. 26.Change in %EI between 14 and 28 days in a) 45% stiff b) 65%stiff and c) 100% stiff groups

Fig. 27. Callus Volume (V_{call}) at 14-day time point

Fig. 28. Callus Volume (V_{call}) at 28-day time point

Fig. 29. Change in callus volume between 14 and 28 days in a) 45% stiff, b) 65% stiff, and c) 100% stiff groups

Fig. 30.Histological appearance of 45% stiff group at a) 14 days and b) 28 days

Fig. 31. Histological appearance of 65% stiff group at a) 14 days and b) 28 days

Fig. 32 .Histological appearance of 100% stiff group at a) 14 days and b) 28 days

Fig. 33a) incorrect position of the MouseFix® plate, with proximal part too far away from the femoral shafta) correct position of the MouseFix® plate, with both ends equidistant from the femur

LIST OF ABBREVIATIONS

BMC	bone mineral content
BMD	bone mineral density
BMP	bone morphogenetic protein
DRF	distal radius fracture
EDTA	Ethylenediaminetetraacetic acid
FE	finite element
GPa	gigapascal(s)
H&E	Haematoxylin and Eosin
HU	Hounsfield Units
IFM	interfragmentary movement
IFS	interfragmentary strain
IHBI	Institute of Health and Biomechanical Innovation
IL	interleukin
IM	intramedullary
KW	Kirschner's wire
M-CSF	macrophage colony stimulating factor
μCT	microcomputed tomography
MIPO	minimally invasive plate osteosynthesis
MSC	mesenchymal stem cell
NBF	neutral buffered formalin
NHMRC	National Health and Medical Research Council
OI	osteogenesis imperfecta

OPG	osteoprotegerin
PMMA	polymethyl methacrylate
PBS	phosphate buffered saline
QUT	Queensland University of Technology
RANKL	receptor activator of nuclear factor kappa-B ligand
ROI	region of interest
Saf-O	safranin orange
TNF	tumor necrosis factor
VEGF	vascular endothelial growth factor
VLP	volar locking plate
WL	window level
WW	window width

STATEMENT OF AUTHORSHIP

To the best of my knowledge, this is an original manuscript and the work contained in this thesis has not been previously submitted for a degree or diploma in any other higher education institution.

I am the original author of this thesis.

QUT Verified Signature

Lidia Koval

01/08/2014

ACKNOWLEDGEMENTS

I would like to express my utmost gratitude to my supervisors, Prof Michael Schuetz, Dr Roland Steck and Dr Devakar Epari, for the opportunity to undertake this project and, more importantly, for their support which helped me see this project through to completion. Dr Roland Steck, a particularly heartfelt thank-you for your patience in answering my endless questions.

MERF staff were invaluable in providing technical assistance in all aspects of animal care and animal surgeries. Thank you, Mark, Siamak and Megan.

IHBI staff assisted me in mechanical testing and preparation of histology slides. Million thanks, Anneliese Dixon, Nicole Loechel and Dr Mia Woodruff.

A/Prof Herwig Drobetz– thanks so much for your critique and your helpful suggestions, which boosted the quality of this work a few notches.

Dr Sarah Whitehouse helped me with statistical analysis which I could not manage on my own. Now I have some idea of how to use SPSS.

To my parents, Lou and Galina Koval, and to my sister, Mariya: thanks for believing in me. I know you all are just as relieved this is finished and you do not have to hear about my Master's anymore.

1. INTRODUCTION

Metaphyseal bone fractures, or fractures in regions primarily consisting of cancellous bone, are among the most common types of fractures observed clinically (Alffram and Bauer 1962, Miller, Grimley et al. 1985, Davies 2001). However, healing of metaphyseal fractures has not been extensively studied, despite their increasing incidence in the aging population. There is a limited general understanding of the steps involved in the healing of cancellous bone, but it has been demonstrated that cancellous bone heals differently than the cortical bone(Jarry and Uhthoff 1971, Uhthoff and Rahn 1981). In this project we used a new experimental murine model to study the influence of the mechanical environment on the healing of metaphyseal fractures. In particular, we used fixation plates of variable stiffnesses for application in the metaphysis of the distal femur of a mouse, and observed the healing outcomes at different time points.

2. LONG BONES

2.1. Basic anatomy and organisation

Bone is a highly anisotropic, viscoelastic material, which continually adapts to changes in its physiologic or mechanical environment. Bone quantity is characterised by the bone's apparent Bone Mineral Density (BMD), as well as by its microarchitecture, its shape and the geometry, and the intrinsic properties of its matrix. On the molecular level, collagen Type I and hydroxyapatite ($Ca_5(PO_4)_3OH$) form the matrix of the bone.

The mineral provides the stiffness and the collagen fibers provide the ductility and ability to absorb energy (i.e., the toughness).

The two types of bone tissue are lamellar and woven bone. **Woven bone** contains haphazardly arranged collagen fibers and is mechanically weaker and less dense than lamellar bone because of its looser packing of the collagen fibers. (McKibbin 1978, Martin, Burr et al. 1998)**.**In adults, it is found at the sites of trauma or disease, most frequently around the fracture site. It is laid down very rapidly, and is the body's attempt to patch up a defect in bone continuity, e.g. resulting from a fracture. Woven bone tissue is the only type of bone tissue which can be formed *de novo*.

Lamellar bone is an orderly array of the bony matrix. It forms from the pre-existing bone tissue, or after the remodelling of woven bone. Lamellae are bands or layers of bone generally between 3 and 7 μm in thickness(Cruess and Dumont 1975, Claes, Wilke et al. 1995). Lamellar bone organisation varies with the bone architecture, discussed in the next section.

2.2. Cortical and cancellous bone

The two principal ways lamellar bone can be organised in a long bone are **cortical** (compact) and **cancellous** (trabecular or spongy) bone. In **cortical** bone, lamellae are arranged into a series of concentric rings around the central tunnel, containing a blood vessel (Haversian canal) (**Fig. 1**). This organisation constitutes an **osteon**, and is a basic unit of cortical bone.

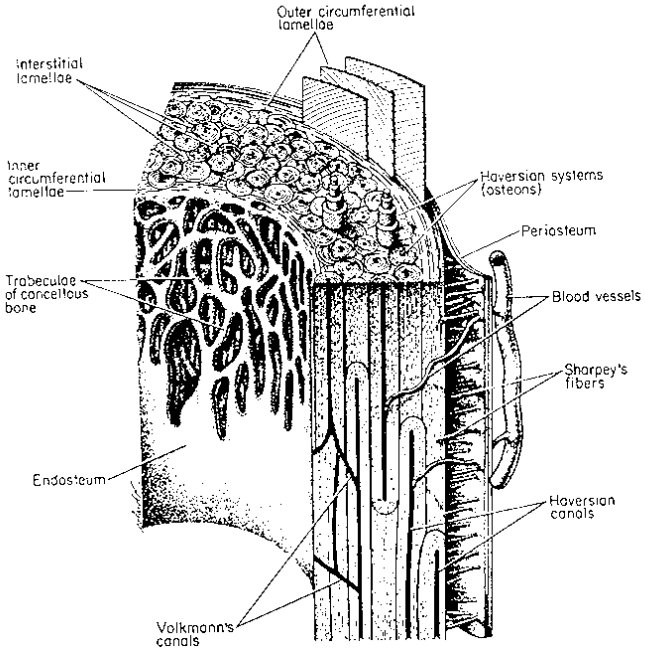

Fig. 1.Organisation of cortical and cancellous bone (Yingling 2008)
(URL:http://academic.brooklyn.cuny.edu/physed/yingling/bone/Structure/Cortical/graphics/bonestructure.gif accessed 05/06/2013)

There are minimal gaps between adjacent lamellae, making cortical bone very dense and resistant to compression. Cortical bone is found mainly in the shaft of long bones, and accounts for 80% of the total mass of an adult skeleton. **Cancellous** bone is, too, composed of lamellar bone, but lacks the Haversian system orientation of the cortical bone. A basic unit of cancellous bone is a trabeculae, which conceptually resembles an unfolded osteon, with lamellae lying parallel. Trabeculae are arranged according to mechanical needs of the bone, and are able to change their orientation in response to the external load on the bone through remodeling (Weinera, Trauba et al. 1999). They are thickest along planes of compression, and thinnest along tension lines. Together, trabeculae form an interconnecting mesh structure, known as trabecular

network, giving cancellous bone its honey-comb appearance(Cruess and Dumont 1975, Dimitriou, Tsiridis et al. 2005).

The composition and material properties of cancellous and cortical bone tissue are the same, and it is their structural differences which confer the particular properties of each type(Weinera, Trauba et al. 1999, Helgason 2008, RISystem 2009). Cancellous bone is more compliant than cortical bone and it is believed to distribute and dissipate the energy from suddenly applied articular contact loads. It accounts for the remaining 20% of total bone mass but has nearly ten times the surface area of compact bone. Its porosity is 30–90%, and has a higher rate of metabolic activity and remodeling then cortical bone. Cortical bone is denser, with 10% porosity, and has a greater compressive strength and greater modulus of elasticity than cancellous bone. As mentioned earlier, the three-dimensional organisation of trabecular network is one of the determinants of bone quality, playing an important role in its resistance to fractures (McKibbin 1978).

2.3. Regions of the bone

The main regions of the long bone are **epiphysis, metaphysis** and **diaphysis (**Fig **2).** The epiphysis is the rounded end of the bone near joints, and contains mainly trabecular bone. The diaphysis is the long, tubular portion, filled with bone marrow, with cortical bone forming the walls of the shaft. The metaphysis is a sub-region of the diaphysis, containing a higher proportion of trabecular bone compared to the rest of

diaphysis, and is located adjacent to the epiphyseal growth plate in an immature bone (Newton and Nunamaker 1985, Marks and Hermey 1996).

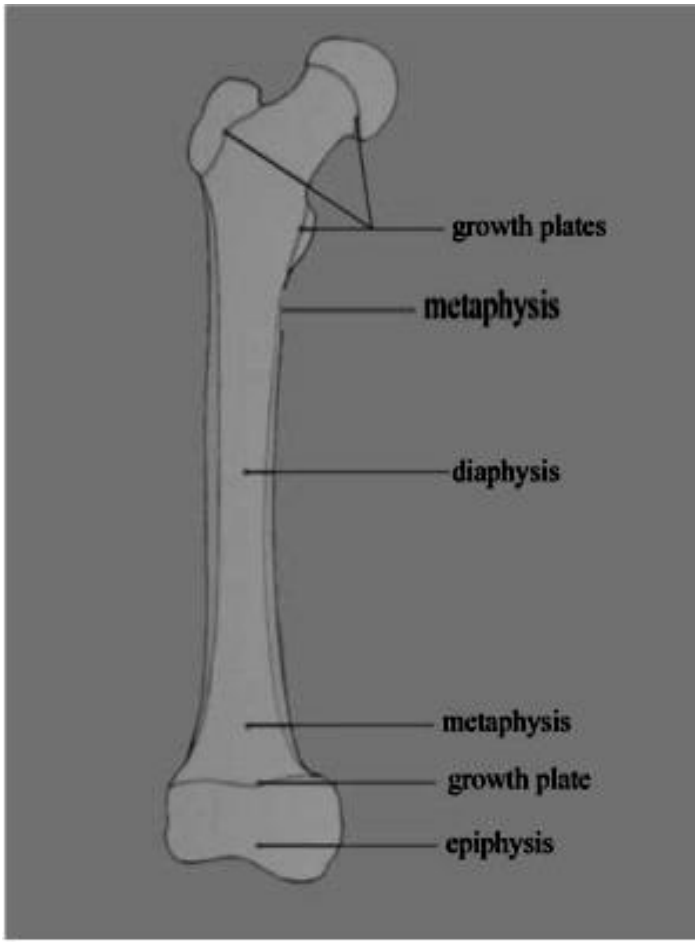

Fig.2. Classification of bone regions on the example of a femur
(URL: www.worldscibooks.com/etextbook/5695/5695_chap01.pdf)

2.4. Periosteum and endosteum

The external surface of a long bone is enveloped by the **periosteum**, with the exception of its articular surfaces, which are covered with articular cartilage. The periosteum is a type of connective tissue developed from mesodermal cells during the

embryonic development. It is tightly attached to various bone surfaces through Sharpey's fibres, forming a thin but very tough membrane(Rauch, Neu et al. 2001). Blood vessels and nerve fibers permeate the outer layer of periosteum (**Fig. 3**). The periosteum allows for bone growth in width. In children, the periosteum is thick and loosely attached to the cortex, allowing for rapid production of new bone. In adults, the periosteum is thinner, adherent to the cortex, and less metabolically active. Periosteum consists of an outer fibrous and an inner layer (Marks and Hermey 1996). The superficial portion of the outer layer is highly vascularised and is a significant contributor to the blood supply of bone and even skeletal muscle. It contains fibroelasticfibres, which frequently serve as the sites of periosteal tendon attachment. The inner layer is called the **cambium**, drawing a parallel with trees, whose inner cambium layer is responsible for appositional growth and the distinctive ring pattern seen in cut logs. It is richly populated by mesenchymal progenitor cells, osteoblasts and fibroblasts, and thus is the essential periosteal component responsible for bone growth(Dwek 2010, Aaron 2012). Pluripotent mesenchymal cells of cambium can be committed to either a chondrogenic or osteogenic lineage(Periosteum, Frey et al. 2013). Periosteum plays an important role in bone repair, and when it is stripped off in the course of a surgery, the healing of bone defects and surrounding soft tissues is seriously compromised(Fan, Bouwense et al. 2010). It is a primary source of the stem cells (Arnsdorf, Jones et al. , Hutmacher and Sittinger 2003) and studies have shown that no cartilage was produced in the fracture callus and fracture healing was delayed if the surrounding periosteum was removed (Hall and Jacobson 1975). Another function of periosteum in bone repair is production of bone morphogenic proteins (BMPs), which drive stem cells

differentiation after the injury(Bostrom 1998). Periosteal sparing is central to the concept of ***"biological osteosynthesis"*** in which the soft tissues adjacent to the fracture site, together with their vascular supply, are preserved, thus accelerating bone repair (Perren 1979). In order to maintain adequate cortical perfusion and normal function of osteoprogenitor cells at the fracture site, it is therefore imperative to limit periosteal stripping during orthopaedic procedures (Utvåg, Grundnes et al. 1996, Mercurio, T et al. 2012). **Endosteum** is an internal membrane, lining the walls of the medullary cavity. Similar to periosteum, it contains osteoprogenitor cells, and provides a functional surface for bone remodeling (**Fig. 3**)(Cruess and Dumont 1975, Frost 1989,Marks and Hermey 1996).

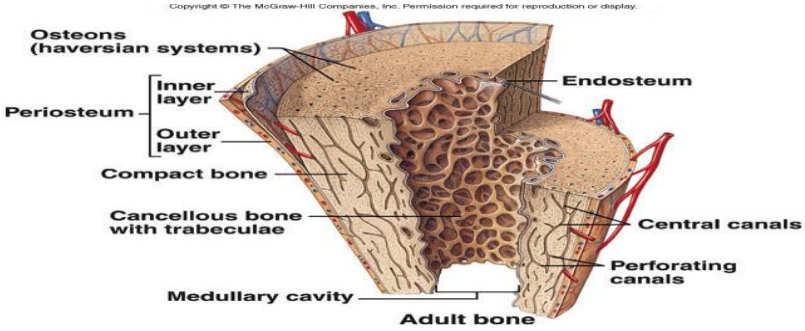

Fig. 3.Periosteum and endosteum(Uzwiak 2013)
URL: http://www.rci.rutgers.edu/~uzwiak/AnatPhys/APFallLect8_files/image003.jpg accessed Jun 12, 2013)

2.5. Blood supply

Cortical and cancellous bone have different blood supplies. In an osteon of cortical bone, concentric lamellae converge around a central (Haversian) canal, containing a blood vessel, a nerve, and a lymphatic. A typical osteon has a diameter of 200 micrometers, which means each cell of the cortical bone is no more than 100

micrometers from the blood supply. The vessels of different Haversian canals are connected with each other, with the bone marrow and periosteum via Volkmann's canals, obliquely spanning the length of the bone from periosteal and endosteal surfaces (**Fig. 4**).

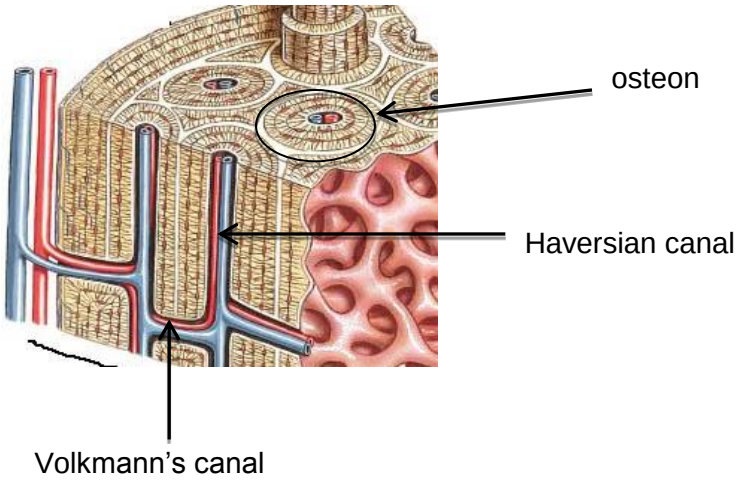

Fig. 4. Blood supply to the cortical bone
(URL:http://test.classconnection.s3.amazonaws.com/124/flashcards/80124/jpg/micro_structure_of_bone.jpg accessed Jun 13, 2013)

Cancellous bone has a larger surface area than cortical bone, and cells are directly exposed to the rich vascular supply of bone marrow, filling the sinusoidal inter-trabecular spaces(Tondevold and Eliasen 1982, Einhorn 2005, Cook and Zioupos 2009). Essentially, bone surrounds blood in the cortical bone, while blood surrounds bone in the cancellous bone, reaching its anatomical destination more directly. Cells of cancellous bone are never far from the surface, thus, there is no need for the complicated Haversian systems. The rate of blood flow in the cancellous bone is also remarkably higher than that in the cortical bone, presumably because of increased energy demands of the cancellous bone, undergoing constant remodeling (WJ 1968, Morris and Kelly 1980, Tondevold and Eliasen 1982).In addition, some studies suggest that local haemodynamic conditions in different parts of the bone are intimately related

to local vascular factors, exerting a directcontrol over local osteogenesis and repair (Brookes 1974). It has been argued that a stimulus to bone formation is provided by a decrease in O_2 levels(Goldhaber 1961), and that cancellous trabeculation is increased in the environment of venous obstruction, or low CO_2 levels (Brookes 1974). However, more recent studies, elucidating the role of local vascular factors in formation of each bone type, and its overall significance for osteogenesis, are currently lacking.

Diaphyseal cortical bone is supplied by the nutrient artery, capillary network in Haversian canals, and medullary vessels. **Nutrient arteries** enter the nutrient foramen near faster-growing epiphysis and pass obliquely towards slower-growing epiphysis. They supplythe marrow cavity and inner 1/3 of the cortex, and their ascending and descending branches anastomose with terminal metaphyseal vessels. The longitudinal network of capillaries in Haversian canals supply the middle 1/3 of the diaphyseal cortex, while transverse capillaries of Volkmann's canals facilitate the flow in and out of the longitudinal system and connect endosteal and periosteal vessels. The flow is primarily centrifugal (in to out) in mature bone, but can reverse depending on physiological conditions. **Medullary arterioles** penetrate across the entire thickness of the cortex, providing it with second source of blood supply. This dual blood supply enables fracture healing after both medullary reaming and periosteal stripping**. Periosteal arterioles** supply the outer 1/3 of the cortex via through vessels of the cambium, but no direct afferent blood vessels exist to mature bone from loosely attached periosteum. They anastomose with skeletal muscle blood network, which becomes its sole blood supply if the periosteum is stripped from the bone during surgery.

3. FRACTURE HEALING

Grossly, the main consequence of a long bone fracture is the loss of its physical continuity. On the microscopic level, the bone also suffers a disruption of its inner biomechanical environment. The aim of bone healing is to restore the integrity of the bone by production of new bone at the site of injury. Whether the bone returns to its original shape and regains its strength depends both on the external factors and on the host's own health. To study the effects of the external environment independently, the host factors have to be controlled by the selection of study animals, which should be as physically similar as possible. In this study, all subjects were of the same strain, breed, age, and sex, and the stability of the external environment was varied with the application of fixators of different stiffness.

3.1. Stages of healing

Any fracture repair proceeds through a characteristic sequence of events, identified as the overlapping stages of inflammation, proliferation, consolidation and remodeling **(Fig. 5).** Past research focused mainly on the healing of fractures in the diaphyseal region of the bone, which consequently is currently best understood. It has been suggested the metaphyseal fracture healing proceeds in a different manner, but the main principles remain the same for both types of bone (Claes, Reusch et al. 2011).

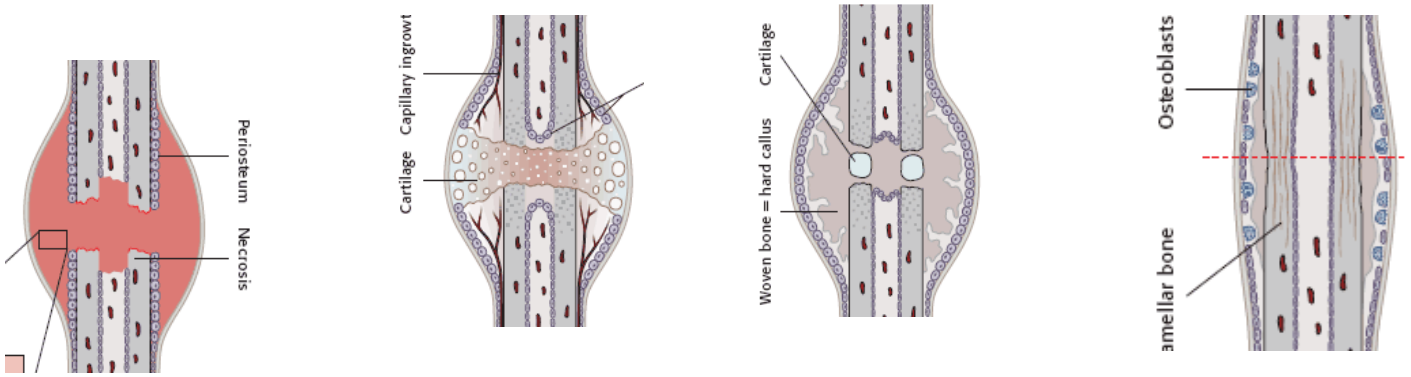

Inflammation **Proliferation** **Consolidation** **Remodeling**

Fig. 5. Stages of bone healing
(adapted from AO Foundation "Biology of Fracture Healing" (Rüedi, Buckley et al. 2007))
https://www2.aofoundation.org/wps/portal/surgery accessed 6/06/2013)

The **inflammation** stage (**Fig. 6**) begins immediately after the traumatic event, and lasts for 2-3days in small animals. A prolonged inflammatory phase is undesirable, as it is associated with delayed angiogenesis (Schmidt-Bleek, Schell et al. 2012). As a result of ischemia following vascular damage, the fractured ends of the bone undergo necrosis, eliciting an intense acute inflammatory response. Blood leakage leads to the formation of ahaematoma, which lifts the periosteum, initiating a cascade of pro-inflammatory molecules. The haematoma also provides a template for subsequent callus formation. Activated neutrophils and macrophages remove necrotic material, induce extracellular matrix synthesis, and recruit other pro-inflammatory molecules, such as tumour necrosis factor-a (TNF-α). TNF-α induces interleukins 1 and 6 (IL-1 and IL-6) to stimulate mesenchymal stem cells (MSC) differentiation into either chondroblasts or osteoblasts, depending on the type of bone healing. Platelets, activated by the haematoma, release growth and differentiation factors for the induction of ossification (Marzona and Pavolini 2009).

Angiogenesis begins during the inflammation stage and continues to the consolidation stage of healing. Two main molecular pathways regulate the

revascularisation, an angiopoietin-dependent pathway, and a vascular endothelial growth factor (VEGF)-dependent pathway, with the input from the acute phase reactants IL-1 and IL-6 and TNF-α(Einhorn 2005). The VEGF-dependent pathway dominates, promoting both the branching of the existing vessels (angiogenesis) and formation of the new vascular plexi from MSCs (vasculogenesis).

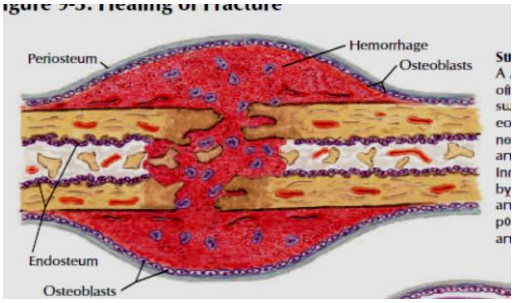

Fig. 6. Stage I: Inflammation
(adapted from Green et al(Greene 2005))

During the inflammation stage, there is a large haematoma, stabilizing the fracture site, with widespread vasodilation causing acute oedema (Cruess and Dumont 1975). The immediate ends of the fracture are deprived of their nutrition and die. Replacement of the primary haematoma with a fibrin-rich granulation tissue marks the beginning of the **proliferation** stage (**Fig. 7**), characterized mainly by endochondral ossification at the fracture site and intramembranous ossification at the periosteal edges. Intramembranous ossification occurs in the periosteum immediately adjacent to the fracture ends. In this process, mesenchymal cells develop into osteoblasts, and new bone is laid down directly on the existing bone with minimal or no cartilage intermediary [5]. The process of endochondral ossification leads to formation of the soft cartilaginous callus, which undergoes mineralisation and resorption before becoming solid bone. The medical term “callus” means newly produced bone, filling the defect between the two

bony fragments. This peripheral callus forms on the external surface of the bone and under the periosteum. It grows rapidly, and it functions as a “bypass” in stabilising the fracture site(Merloz 2011). In small animal models, the peak of soft callus formation occurs 7-9 days after the fracture(Claes, Heigele et al. 1998, Einhorn 1998). The function of callus is to decrease movement at the fracture site, which both reduces pain and allows bone to retain its shape as it progresses to the next stage of healing. The amount of callus formed depends on the amount of MSCs recruited to differentiate into chondroblasts, which, in turn, depends on the mobility within the fracture site.

The healing of the bone following fracture is a combination of both types of ossification, but it is the biomechanical environment at the fracture site determining which type will predominate. Studies suggest that weight bearing and micromotion at the fracture site stimulate copious callus production, and therefore encourage endochondral ossification, whereas rigidly fixed fractures heal with little or no callus, or primarily by intramembranous ossification (Claes, Heigele et al. 1998, Schell, Epari et al. 2005, Epari, Schell et al. 2006)

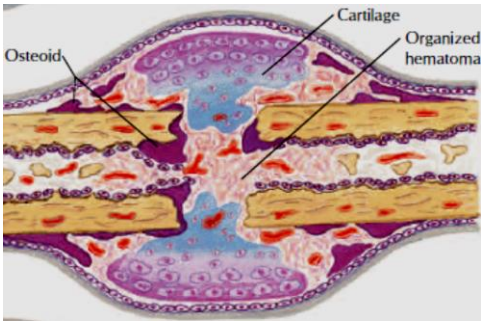

Fig. 7.Stage II: Proliferation(adapted from Green et al(Greene 2005))

The **consolidation** stage (**Fig. 8**) leads to union of the fractured endings by replacement of cartilage by osseous tissue, with the peak of hard callus formation

occurring around day 14 in small animals models (Einhorn 1998). To some extent, this stage mimics embryonic bone development. This transition of cartilage to bone is a result of the complex interplay between macrophage colony-stimulating factor (M-CSF), receptor activator of nuclear kappa B ligand (RANKL), osteoprotegerin (OPG) and TNF-α. As the chondrocytes mature, their extracellular matrix calcifies, trapping blood vessels. The combination of ensuing hypoxia and TNF-α activity leads to chondrocyte apoptosis. Meanwhile, the calcified matrix acts as a nidus for further mineral deposition. Eventually, bone rigidity is re-established following incorporation of the apatite crystals for the formation of calcified cartilage, and fusion of the central hard callus at the edges of the fracture (Einhorn 2005).

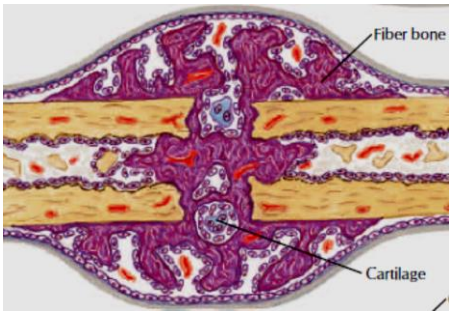

Fig. 8.Stage III: Consolidation
(adapted from Green et al (Greene 2005))

The new bone does not possess the same strength as the normal bone because of the lack of a preferred orientation of the collagen fibres in the matrix. Bone strength is regained in the final **remodeling** stage of repair (**Fig. 9**), where the newly-formed bone is gradually converted to the lamellar bone with trabecular orientation depending on the mechanical demands at the fracture site (Shefelbine and al 2005).

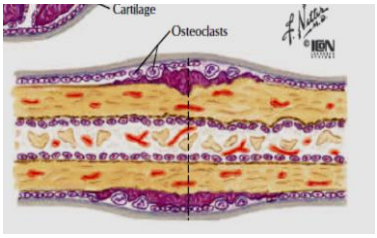

Fig. 9.Stage IV: Remodelling
(adapted from Green et al(Greene 2005))

4. METAPHYSEAL FRACTURES

Fractures of the metaphysis are among the most common fractures observed clinically. Studies of metaphyseal bone repair are sparse, partly because until recently, there were no well-designed fracture models targeted to study them. Thus, the importance of the biomechanical conditions in the healing of these fractures came under scrutiny only in the last decade.

4.1. Epidemiology

Metaphyseal fractures have bimodal distribution, peaking in adolescents and in elderly females, with metaphyseal fractures of the distal forearm comprising more than two-thirds of all fractures of the forearm bones (Alffram and Bauer 1962).

In toddlers, these fractures are often a hallmark of non-accidental injuries (Kemp, Dunstan et al. 2008). They are usually found at the end of the long bones and at the terminal portion of the ribs, and are the result of the repeated torsional or shearing forces (twisting the child's arm or leg), or thoracic compression with front-to-back force (such as from grabbing a child by the sides and shaking). These injuries are known among radiologists as "corner", or "bucket-handle" fractures (Kleinman 1998), and are

virtually pathognomonic for child abuse, after genetic and metabolic causes have been excluded. Risk factors in pre-adolescent children include low dietary calcium intake, low bone mineral density (BMD) and bone mineral content (BMC), and genetic and metabolic disorders. These children tend to have multiple fractures, with a first fracture before adolescence. In adolescents, fractures of the distal forearm peak around the onset of pubertal growth spurt (Khosla, Melton et al. 2003). Interestingly, obese children are more likely to sustain multiple fractures of the distal radius. Gaulding et al argues that not only do they fall with more force than lighter individuals, but their BMD and BMC at the distal radius is smaller than that of lean children(Goulding, Jones et al. 2001). Other authors think that the increased demand for calcium at the time of maximal longitudinal bone growth leads to the transient increase in bone porosity. Others postulate that the process known as **metaphyseal inwaisting** is to blame for the site-specific osteopenia in the metaphyses of the long bones in the period of peak growth. Metaphyseal inwaisting is a process that occurs during long bone growth and remodelling of epiphyses. As the growth plate proceeds in a distal direction, a section of newly created metaphyseal bone continues to decrease its diameter by periosteal resorption until it has reached the cross-sectional size of the diaphysis. This process leads to a temporary thinning of the cortical bone, which makes it more susceptible to fracture, even with light trauma(Rauch, Neu et al. 2001, Wang, Wang et al. 2010). This temporary weakness, in combination with an active lifestyle of a typical adolescent, leads to increased incidence of distal forearm fractures. In summary, the development of strength at the distal radius in adolescents lags behind the increase in factors, challenging bone stability during the fall.

One out of 3 adults aged 65 and over fall each year, and most fractures among older adults are caused by falls (Bell, Talbot-Stern et al. 2000, Jager, Weiss et al. 2000,Hausdorff, Rios et al. 2001). Risk factors for falls increase with age, and include decreased muscle strength, delayed reflexes, slower reaction time, impaired vision, infrequent walking, and use of diuretics and psychotropic drugs. In general, post-menopausal women are both at the highest risk of falling and sustaining a fracture after a fall (Alffram and Bauer 1962, Miller, Grimley et al. 1985, Earnshaw, Cawte et al. 1998,Davies 2001). Women also live longer than men, and often reside alone in a cluttered household where they are at risk of tripping and falling. A steady rise in fracture incidence after menopause may reflect osteoporosis and increased risk of falling as the main predictors of fracture in the older female population. The fact that the injury a result of moderate energy trauma in 3 of 4 women 50 years and older and that the incidence of displaced fractures is highest among the oldest women may reflect that low bone density increases the risk of fracture (Miller, Grimley et al. 1985). In addition, the risk of falling is increased after menopause among women, possibly due to poor reaction time and reduced muscle strength (Miller, Grimley et al. 1985, Davies 2001).

With age, there is a shift in the cell types populating the periosteum, in particular an increased fractional number of osteoclasts in the metaphysis, indicating increased resorptive activity of cortical bone in metaphyseal areas. The result of this degenerative process is progressive fragility of cancellous bone, which accounts for the higher incidence of the distal radius fractures in older women in the metaphyseal region (Alffram and Bauer 1962).

4.2. Metaphyseal fractures healing

Fracture healing proceeds differently in metaphyseal and diaphyseal bone, owing to the structural differences between the two types of bone (Shefelbine, Augat et al. 2005, Egermann, Heil et al. 2010). The diaphysis is tubular, with a thick layer of compact cortical bone forming its wall and bone marrow filling the hollow medullary canal. In contrast, the metaphysis contains abundant trabecular bone, but the cortical bone envelope thins here relative to the diaphysis.

In most cases, diaphyseal fractures heal mainly through **endochondral** ossification, with deposition of cartilaginous callus preceding the formation of solid bone (**Fig. 10**). Metaphyseal fractures tend to heal through **intramembranous** ossification, with new trabeculae arising directly from the existing ones (**Fig. 11**). Instead of intermediary callus, the fracture gap is initially filled with woven bone, an immature type of bone tissue, which is less dense than normal lamellar bone due to irregular and random packing of type I collagen fibers (Martin and Burr 1989). This bone type is then converted to lamellar bone, with no fibrocartilaginous callus in the interim. It has been suggested that the large, biologically active surface of the trabecular bone eliminates the need for intermediary callus by providing a reservoir of mesenchymal cells for osteocyte production (Thompson, Miclau et al. 2002, Claes, Reusch et al. 2011).

Fig. 10.Endochondral ossification with callus formation (adapted from Epari et al(Epari 2006)

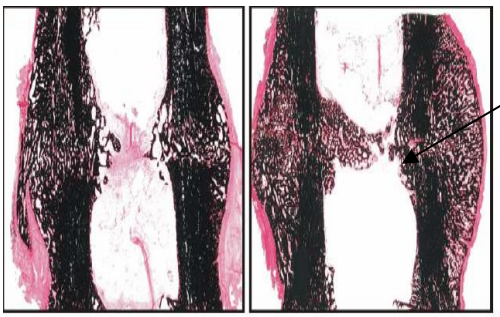

Figure 3-13 The callus histology (Safranin Orange/von Kossa) after 9 weeks healing shown under rigid (left) and semi-rigid (right) fixation.

Fig. 11. Intramembranous ossification with direct ossification across the fracture gap (adapted from Epari et al) (Epari 2006)

It has been shown that metaphyseal fractures heal faster than diaphyseal fractures and that they have a lower incidence of non-union (Aronson and Shen 1994). Bone formation in the metaphyseal region is significantly enhanced by the vast surface area of trabecular boneand direct access of the trabecular mesh to the rich vascular supply of the bone marrow. The increased rate of blood flow in the metaphyseal region also contributes to the faster bone formation and remodelling. In bone lengthening

studies, the metaphyseal region demonstrated earlier new bone formation, remodelling, and mineralisation than the diaphyseal site, particularly during the consolidation stage. Subsequent mechanical testing confirmed stronger regenerate bone in the metaphyseal gap (Aronson and Shen 1994). In young people, the high osteogenic potential of the metaphyseal periosteum is indicated by the high number of stromal cells present, capable of differentiating into multiple mesenchymal cell lineages including osteoblasts and chondrocytes (Fan, Bouwense et al. 2010).

4.3. Principles of treatment of metaphyseal fractures

The aim of treatment of a metaphyseal fracture, as for any fracture, is a successful reduction with subsequent immobilization, either in a cast or with an appropriate fixation device (Robinson, Hill et al. 2003, Yang, Tzeng et al. 2006, van Aaken, Beaulieu et al. 2009, Bales and Stern 2012). The treatment can thus be operative or non-operative, depending on the nature of the fracture and on the surgeon's preference.

There are different methods of operative treatment of metaphyseal fractures. Distal radius fractures (DRFs) can be treated by fixation with Kirschner wires (K-wires), bridging and non-bridging external fixators, and volar or dorsal (locking) plates. Distal femur fractures are managed with plate fixation or locked intramedullary (IM) nails. In case of DRFs, there is evidence that the radiological results with operative treatment are better than with non-operative treatment (Diaz-Garcia, Oda et al. 2011). The long-term functional results of distal radius fractures are not seen to be significantly different, regardless of the treatment method (Young and Rayan 2000,Egol, Walsh et al. 2010,Jupiter and Marent-Huber 2010). However, in view of increased patient

expectations, better implants and operative techniques, and faster rehabilitation times, non-operative treatment is losing popularity among surgeons and patients alike. Patients, who sustain a distal radius fracture, can expect more quality-adjusted life years after operative treatment than with conservative treatment by immobilization, and the long-term gain of painless years outweighs the short-term risks of surgical complications (Koenig, Davis et al. 2009).Stiff volar locking distal radius plates (VLDRPs) have become a popular choice among surgeons for fixation of unstable metaphyseal fractures of distal radius, and are a preferred method for operative management of DRFs, resulting in excellent to good results in the majority of patients (Nana, Joshi et al. 2005, Smith and Henry 2005). The concept has been developed in 1996 by Drs Kutscha-Lissberg and Drobetz in Neunkirchen General Hospital, Austria, and the plates have been produced by Synthes® since 1997. VLDRP provide stable internal fixation and allow early function by successfully immobilising osteopenic bone, with an average time to radiographic union of 7.1 weeks(Orbay and Fernandez 2004). The plates reliably maintain the intraoperatively achieved reduction (**Fig. 12**) and, importantly, are the only treatment modality which allows immediate mobilization of the wrist without traditional 6-weeks fixation in a cast or an external fixator(Knox, Ambrose et al. 2007). It has been shown in clinical studies that the intraoperative reduction achieved with volar locking plates can be maintained throughout the bone healing process if the plates are positioned close to the articular joint line (Drobetz, Bryant et al. 2006). Treatment with K-wires and external fixators is a demanding form of treatment, both on the patient and the treating surgeon. Patients must return for follow-ups and cast changes at least once a week and, in the case of treatment with external fixators,

the pin sites need regular cleaning and are prone to infection and loosening. In addition, pinning with K-wires results in a less stable construct than volar plating, with the average movement across the fracture site of 2.5 mm with pin fixation and only 1.1 mm with plate fixation, and “notable degree of slipping after repeated testing” (Knox, Ambrose et al. 2007).

Fig. 12. Volar Locking Distal Radius Plate (VLDRP) applied to the distal radius(author’s archive)

The best option for the surgical treatment of distal tibial metaphyseal fractures is still unclear. Plates require a wide soft tissue dissection that carries risks of infection, wound breakdown, and devitalisation of the surrounding tissue. The technique of minimally invasive plate osteosynthesis (MIPO) has been developed in recent years(Oh, Kyung et al. 2003, Toms, McMurtie et al. 2004). The main advantage of this technique is minimising the risks of wound dehiscence and of periosteal stripping. Likewise, intramedullary (IM) nailing has gained popularity in the treatment of tibial diaphyseal fractures. However, this method has its own set of complications, such as malreduction,

malunion, implant failure, and fracture propagation into the ankle joint. Studies show that both methods produce similar functional results, though the time to union was shorter with nailing than with MIPO plating (Yang, Tzeng et al. 2006).

4.4. Stiff vs Flexible fixation

The research concerning the influence of the mechanical environment on the healing of metaphyseal fractures is limited. Jarry and Unthoff (Jarry and Uhthoff 1971) conducted a series of experiments where they examined trabecular healing under stable and unstable conditions in rats. They concluded that instability and gross displacement of metaphyseal fractures leads to formation of an external fibrocartilaginous callus, or healing primarily by endochondral rather than intramembranous ossification. Later experiments by Unthoff and Rahn(Uhthoff and Rahn 1981)confirmed these findings, suggesting that movement at the fracture site changes the usual healing pattern of metaphyseal bone from intramembranous to the combination of intramambranous and endochondral ossification.However, the biomechanical conditions were not controlled or defined sufficiently in these series. Uusitalo and colleagues (Uusitalo, Rantakokko et al. 2001) conducted a study in 2001, where they produced a circular defect in the cortical bone in the distal femur of the mouse, with no subsequent fixation, and found that it healed by the combination of intramembranous and endochondral ossification. Again, the biomechanical conditions were not controlled in this study. In 2008, Claes et al (Claes and Cunningham 2009) piloted a project where they investigated the healing of the partial osteotomy in the distal femur of the sheep, where the interfragmentary movement (IFM) was determined

by the thickness of the spacer plate. They found that the amount of callus formation in the osteotomy gap was directly related to the amount of IFM movement in these regions under load. Claes later repeated this study (Claes, Reusch et al. 2011) with a larger number of subjects and under controlled biomechanical conditions, and found that the optimal IFM strain for fracture healing falls between 5 – 20%. In 2011, Han and colleagues (Han, Zhang et al. 2012) trialled a rabbit metaphyseal fracture model by splitting the medial tibial plateau and rigidly fixing it with compression screws. They found that fracture healing proceeded via direct intertrabecular proliferation, with no evidence of external callus formation in the fracture area which supports the theory that absence of movement at the fracture site will lead to direct end-to-end healing of the fracture, with little intermediate callus. Strictly speaking, the medial tibial plateau is not a metaphyseal bone, but this region of the tibia contains mostly trabecular bone, as does the metaphysis, and it is a reasonable assumption that the findings of the study can be extrapolated to bone in metaphyseal regions. In 2011, Histing and colleagues (Histing, Klein et al. 2012) performed a series of experiments where they studied the healing of the rigidly fixed distal femur osteotomy in a mouse, and found that it healed exclusively through intramembranous ossification. Our experiment expands on this study by introducing variability of stiffness of internal fixators.

Table 1 summarises the existing research on the healing of metaphyseal fractures.

Author	Method	Animal	Fixation	Control of IFM	Number of animals	Healing time	Results
Jarry 1971	Distal femur osteotomy	Rat	Rigid and flexible	None	18	8 weeks	Intramembranous healing under stable conditions, fibrous tissue formation under unstable conditions
Uhthoff 1981	Partial and complete osteotomies in distal femur	Rat, rabbit, dog	Rigid and flexible	None	20	4 weeks	Intramembranous ossification with no external callus under stable conditions. Endochondral ossification with fibrocartilage and delayed union under unstable conditions
Uusitalo 2001	Circular cortical defect in the distal femur with K-wire, no subsequent fixation	Mouse	No fixation	None	106	6 weeks	Defect healing by combination of intramembranous and endochondral ossification
Claes 2008	Partial osteotomy in the distal femur with spacer insertion in the gap	Sheep	Variable flexibility	Variable thickness of the plate in the osteotomy gap	2	8 weeks	Intramembranous ossification under stable conditions, fibrocartilage and delayed healing under unstable conditions
Stuermer 2010	Proximal tibial osteotomy with T-plate fixation of the fracture	Rat	Rigid	None	43	5 weeks	Estrogen and raloxifene improve fracture healing in osteoporotic bone after osteotomy and stable internal fixation
Claes 2011	Partial osteotomy in the distal femur with spacer insertion in the gap	Sheep	Variable flexibility	Variable thickness of the plate in the osteotomy gap	12	8 weeks	Intramembranous ossification with <5% of IFM strain, combination of endochondral and intramembranous ossification between 5 and 20% of IFM strain, and fibrocartilage with non-union with > 20% IFM strain
Han 2012	Tibial plateau osteotomy with compression screw fixation	Rabbit	Rigid	None	18	8 wks	Intramembranous ossification without callus
Histing 2012	Distal femur osteotomy fixed with the plate	Mouse	Rigid	Stiff MouseFix® plates	30	5 weeks	Intramembranous ossification without callus

Table 1. Summary of studies, investigating healing of metaphyseal fractures

5. ANIMAL MODELS OF FRACTURE HEALING AND MOUSEFIX®

5.1. Animal models of fracture healing

In vivo, or animal testing, is an important phase of medical research to predict clinical safety of new medical devices or therapies. Over the past four decades, many improvements have been implemented in design of animal studies, leading to reduction of the number of animals used, while preserving the study effectiveness. Due to the lack of standardization and defined mechanical conditions achievable in small animals, most previous research on the role of mechanical environment on fracture healing has been done on large animals, such as sheep. Similarities of bone structure and biomechanical loads between sheep and humans make ovine models well-suited for pre-clinical evaluation of new implants or treatment strategies (Martini, Fini et al. 2001, Nuss, Auer et al. 2006). However, sheep models are not ideal for studying the underlying molecular biological processes. In general, there is a lack of antibodies and other reagents available for most large animal models compared to rodents. Also, genetic manipulation is easier and more cost-effective in rodents than in sheep. Finally, animal costs can be significant, and having an adequate number of animals can be problematic if large animals are used. Currently, murine models are preferred to study musculoskeletal disorders, and are employed in 21% of all medical research, and in approximately 7% of musculoskeletal research, primarily to study osteoporosis (Turner, Maran et al. 2001). The mouse

genome has been completely decoded (Cox, Ackert-Bicknell et al. 2009) and a large variety of mutated mouse strains are available. Mice are robust animals, which are cheap to buy and to keep. In this experiment, we use the albino mouse, strain Arc:Arc(S)/CD1, which is believed to have a bigger trabecular bone compartment compared to other common research strains. Initial experimental mouse fracture models, which generally consisted of fractures created by 3-point-bending and stabilized with simple intramedullary pinning, lacked the biomechanical definition and control to make them useful for relating the expression of proteins to the biomechanical conditions during fracture healing (Histing 2009). This shortcoming has been addressed through the development of several more appropriate fixation systems for murine fractures (Holstein, Matthys et al. 2009).

5.2. MouseFix® development

In particular, the MouseFix® murine fracture model (AO Research Institute, RISystems, Switzerland) promises to become a standard murine fracture and fixation model (RISystem 2009). This model has been developed by Matthys et al at AO Research Institute (RISystem™, Davos, Switzerland) in 2009. In this model, a femoral midshaft osteotomy is stabilised by internal fixation plates, which are applied during a surgical procedure to the anterolateral surface of the femur. This plate-like internal fixator is available either as a single solid plate, or as two shorter plates, connected by a pair of bridging wires (**Fig.13**). The flexibility of the implant thus can be varied by changing the parameters of the

bridging wires. The plates are fixed to the mouse femur by four self-tapping locking screws with the help of the miniature drill guide and an electrical pen drill set. A micro Gigli saw is then used to create a transverse osteotomy, with gap sizes of 0.22, 0.44, or 0.66 mm. The most important feature of this model is that it allows study the effects of various fixation stabilities on the healing of the bone under defined biomechanical conditions by enabling the selection of different degrees of fixation stability and of different gap widths. The method of plate application and osteotomy creation is reproducible, simple to learn, and well tolerated by the animals (Matthys and Perren 2009).

Varying degrees of stiffness can be achieved by modifying the diameter, the length and the material of the bridging wire. The Trauma Research Group at the Institute of Health and Biomedical Innovation (IHBI) has been instrumental inconducting the mechanical characterization of these implants by finite elements (FE) simulations and experimental validation. Using the FE simulations, it was possible to further develop the model by establishing the equivalent bending stiffness, torsional rigidity and three-dimensional interfragmentary movement of the plates, and to confirm the purported plate stiffness of 100%, 65% and 45%.

In this study, we utilised the option of available rigid and flexible MouseFix® fracture fixation implants to determine the influence of fixation rigidity in the context of metaphyseal fracture healing**.**

Fig.13.MouseFix® plating system for metaphyseal fractures(RISystem 2009)

(URL: www.risystem.com/Standardized_Implant_for_Research/MouseFix_files/meta_MouseFix_SGT.pdfaccessed Jun 10, 2013)

5.3. Use of MouseFix® in medical research

In 2009, Groengroeft and colleagues (Gröngröft, Heil et al. 2009) introduced the newly designed MouseFix® locking plate system with a series of experiments on mice to investigate the relationship between the fixation compliance and healing of midshaft femoral fractures. They traced the differences in healing of the midshaft femoral osteotomy after application of a conventional rigid plate and a newly designed flexible plate, which had the rigidity of ¼ of the conventional plate. Their studies showed that the healing of the rigidly fixed diaphyseal fracture in a mouse resembled that of the rigidly fixed human bone, or intramembranous ossification with trabecular remodelling. In contrast, flexible fixation of the same region resulted in a pattern, similar to the human secondary bone healing, or a mixture of endochondral and intramembranous ossification, with copious intermediary callus formation. This study also showed that the union of fracture fragments was delayed only by a few days in the group, treated with flexible implants, and the callus stiffness, which is one of indicators of bone healing (Hente, Cordey et al. 2003), was comparable in both groups.

In 2010, Claes et al (Claes, Blakytny et al. 2011) determined that for effective metaphyseal bone healing the optimal interfragmentary strain (IFS) falls between 5% and 20%. This amount of IFM not only results in formation of the greatest amount of new bone, but the newly formed bone has thicker trabeculae and higher bone density than bone, formed under other conditions. IFS<5% was

associated with slower healing, lower bone density and primarily intramembranous ossification. These results are expected in healing of fractures under stable conditions. IFS>20% did not prevent healing, but resulted in delayed union of the fracture segments, presumably because persisting fibrocartilaginous callus hindered the end-to-end union of the fractured bone. In summary, the optimal amount of IFM within the fracture gap is between the minimum at which callus production becomes stimulated (5%) and maximum, after which bony bridging becomes compromised (20%). It is not yet clear what induces the change in ossification pattern on the cellular level. However, it has been demonstrated that mesenchymal cell induction begins as early as in the inflammation stage of healing, with TFN-α and interleukin-6 playing a pivotal role in mesenchymal cell differentiation into either chondrocytes or osteocytes (Marsell and Einhorn 2011)**.**In 2011, Steck and colleagues (Steck, Ueno et al. 2011) conducted a study, investigating the relationship between bending and torsional flexibility of the implant and the mechanical strength recovery of the femur in the first 4 weeks of bone healing, using the results of the microCT imaging to interpret their findings. They established that rigidly fixed bones exhibited an earlier return of mechanical strength, compared to the bones stabilised with a compliant implant. Rigid fixation was associated with a small, dense callus and early bridging of the fracture gap (at 14 days), with small subsequent increase in torsional stiffness. In contrast, flexible fixation of the fracture resulted in an abundant periosteal callus of low mineral density and slower bridging of the fracture fragments, but stiffness values continued to

increase after 14 days, as the bridging progressed. These two experiments demonstrated that implant stiffness plays a larger role in murine fracture healing than the fracture gap width (Gröngröft, Heil et al. 2009, Steck, Ueno et al. 2011). However, they only used two types of implants in their studies, and were unable to establish the degree of implant compliance which would optimise fracture healing. Also in 2011, Histing et al (Histing, Klein et al. 2012)performed a series of experiments on mice with a modified version of the MouseFix® locking plate system. Their study concentrated on the healing of fractures in the metaphyseal region of the murine femur, treated with rigid fixation of the fragments. This type of fixation produced an intramembranous ossification pattern of healing, with the new woven bone filling the osteotomy gap and no evidence of external callus. This experiment also claimed that an adapted MouseFix® locking plate is a reliable and reproducible method for studying metaphyseal fracture healing in mice under mechanically defined conditions.

6. HYPOTHESES

6.1. Knowledge gaps

The interest in the relationship between the flexibility of fracture fixation and metaphyseal fracture healing prompted some previous research on the subject. However, some questions remain to be answered. Opinions are divided regarding the influence of flexible fixation and associated movement within the fracture gap on the mode of metaphyseal fracture healing. Secondly, the

relationship between the amount of callus, formed around the healing metaphyseal fracture, and the flexibility of fixation has not been investigated. Finally, it is still not clear whether the recovery of bending stiffness in metaphyseal bone following fracture is the same under stable and unstable healing conditions. The aim of this experiment was to answer these questions.

6.2. Objectives and Hypotheses

The overall aim of this project is to determine the role of fixation stiffness on metaphyseal fracture healing in the mouse under defined biomechanical conditions by using a novel experimental mouse model using the MouseFix® plates of variable stiffness.

The following hypotheses were tested:

1. The implant stiffness affects the bone repair mechanism in metaphyseal bone fracture healing, with stiff implants leading to predominantly intramembranous ossification and more flexible implants leading to mainly endochondral ossification.
2. The amount of callus formation is directly related to the flexibility of internal fixation.
3. The bending stiffness of the healing bones is dependent on the flexibility of the internal fixation.

7. MATERIALS AND METHODS

All procedures followed the Australian Code of Practice for the Care and Use of Animals (NHMRC, 2004)((NHMRC) 2008) and have received approval from the University's Animal Ethics Committee (QUT University Animal Ethics approval number 1100000319).

There were 81 albino mice (C57/BL6) in total, of which nine were used in the pilot study, and the remaining 72 in the current study. There were three study groups of 45% stiff, 65% stiff and 100% stiff fixation, and animals were randomly assigned to one of the groups. Animals were sacrificed at 14 and 28 days postoperatively, which correspond to the early and late stage of healing, respectively.

Table 2 provides a summary of the Materials and Methods in this experiment.

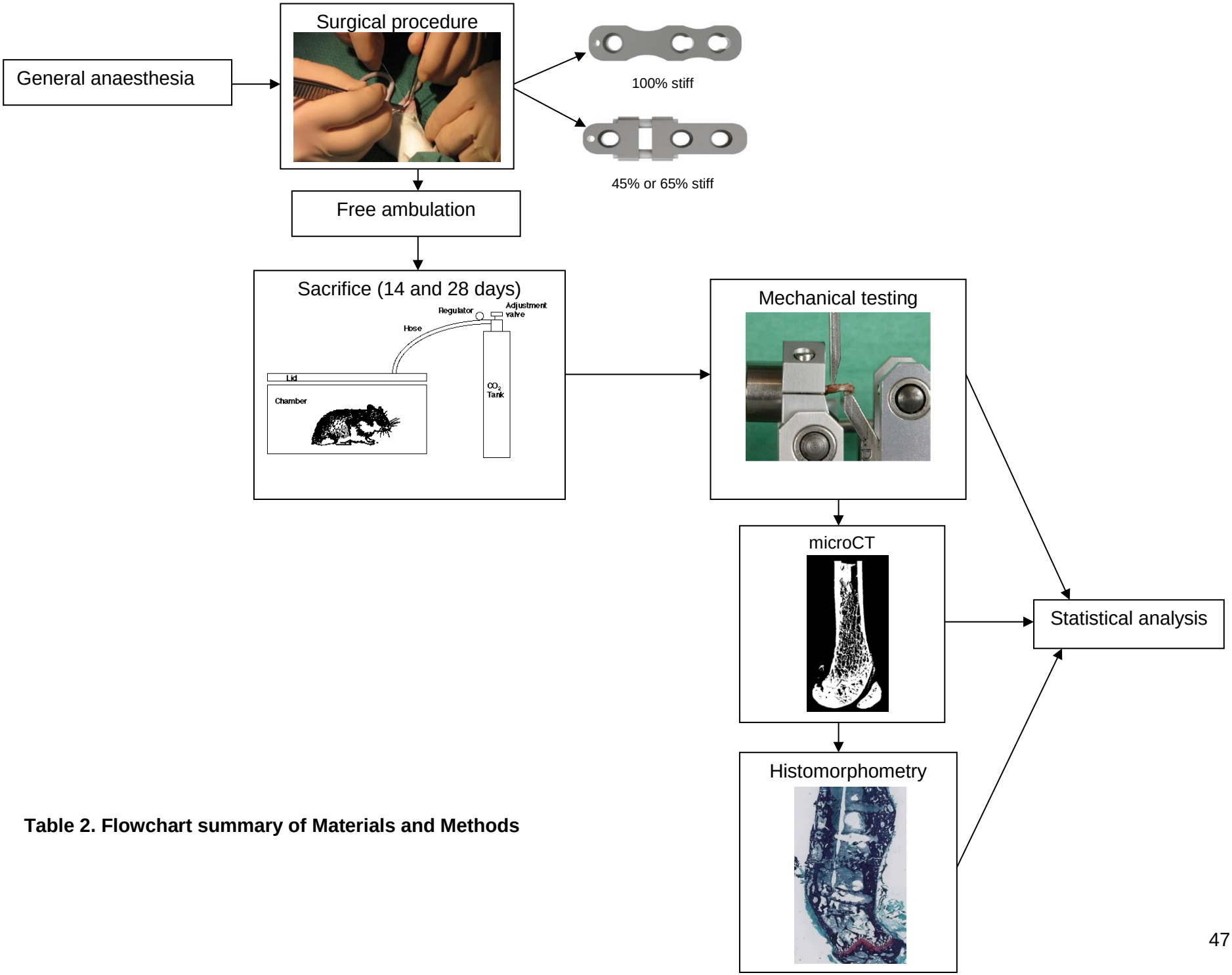

Table 2. Flowchart summary of Materials and Methods

7.1. MouseFix® design

MouseFix® locking plates for studying metaphyseal bone healing in the distal femur of the mouse consists of the titanium plate in a 3-hole configuration. Three plates of different stiffnesses were developed. A “rigid” plate is made of the single solid bar of metal, and a “flexible” plate consists of two short plate segments, connected by a pair of bridging wires, made of a titanium/nitinol alloy. The flexibility of the plate is determined by the thickness and length of the bridging wire (**Fig. 14**). For these implants, bending stiffness is only in out-of-page bending for 100%, 65% and 45% stiff plates, used in this study.

Fig. 14. Two configurations of the MouseFix® plate: a) rigid b) flexible (RISystem 2009)
(URL: http://www.risystem.com/Standardized_Implant_for_Research/RISystem.html accessed Sep 10, 2013**)**

The plates are attached to the bone with self-tapping locking screws, using a drill guide and a battery-operated drill (**Fig. 15**).

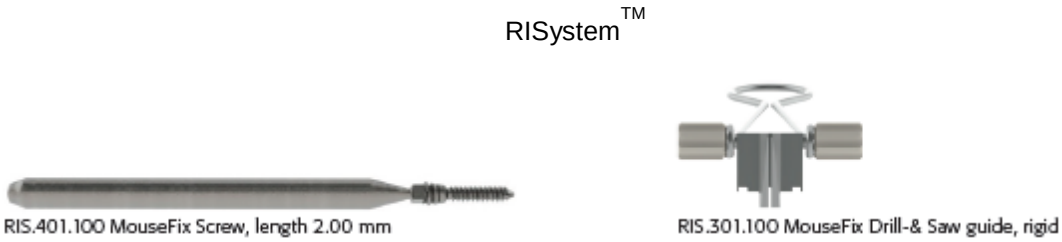

Fig. 15. a) Self-tapping cortical locking screw andb) Drill guide (RISystem 2009)

(URL: http://www.risystem.com/Standardized_Implant_for_Research/RISystem.html accessed Sep 10, 2013**)**

7.2. Surgical procedure

General anaesthesia was achieved and maintained using a combination of 2.5% Isoflurane and oxygen, delivered through a facemask. Animals were monitored closely for signs of respiratory depression, and the rate of gas flow was adjusted accordingly. A single dose of Keflex® (cephalexin) and a single dose of buprenorphine analgesia were administered as an intraperitoneal injection before the surgery. With the mouse in prone position, the animal's left hind-limb was cleaned with Chlorhexidine solution and a longitudinal incision (~10mm) was made over the lateral aspect of the thigh through the skin and fascia lata, extending along the femur to the knee. *Vastus lateralis* and *biceps femoris* muscles were split, and *tensor fascia latae* muscle lifted to expose the distal part of the femur. Care was taken to identify and preserve the sciatic nerve (**Fig. 16**).

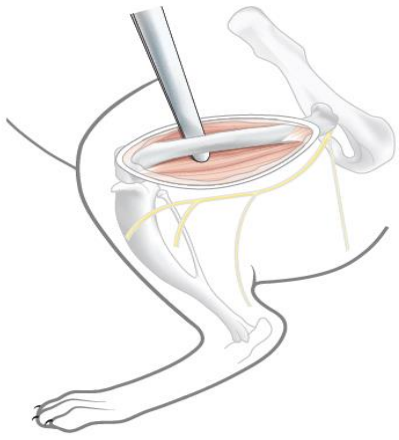

Fig. 16. Surgical approach: preparation of the femur

(adapted from RISystem™, Davos, Switzerland (RISystem 2009))
(URL: http://www.risystem.com/Standardized_Implant_for_Research/MouseFix.html accessed Jun 10, 2013

A piece of Gigli wire was threaded under the femur in medio-lateral orientation. After the femur was prepared, the internal fixation plate of one of the three stiffnesses was applied to the antero-lateral aspect of the distal metaphysis using three locking screws and a trocar pin (**Fig. 17**). A .22mm osteotomy was created in the metaphysis of the bone with a Gigli saw to mimic a simple metaphyseal fracture (**Fig. 18**). The osteotomy produced a fracture gap of .22mm. With the diameter of the mouse femur approximating 2mm (measured by the investigator), the size of the osteotomy is below the recommended limit of 20% of the diameter of the bone (Histing, Garcia et al. 2011).

The surgical site was then cleaned and closed by suturing in layers, and Betadine® ointment was applied to the wound. The animals were allowed to weight bear as tolerated after the procedure. Limiting the implant mass to 1:1000 of the animal mass minimizes uncontrolled loading due to inertia in free ambulation, and conveniently matches the ratio between the mass of a medium-sized femur plate with its screws (65-70mg) and a mass of the average human (75kg).

Fig. 17. Rigid MouseFix®plate, applied to the metaphysis of distal femur
(adapted from RISystem™, Davos, Switzerland (RISystem 2009))
URL: http://www.risystem.com/Standardized_Implant_for_Research/MouseFix.html accessed Jun 10, 2013)

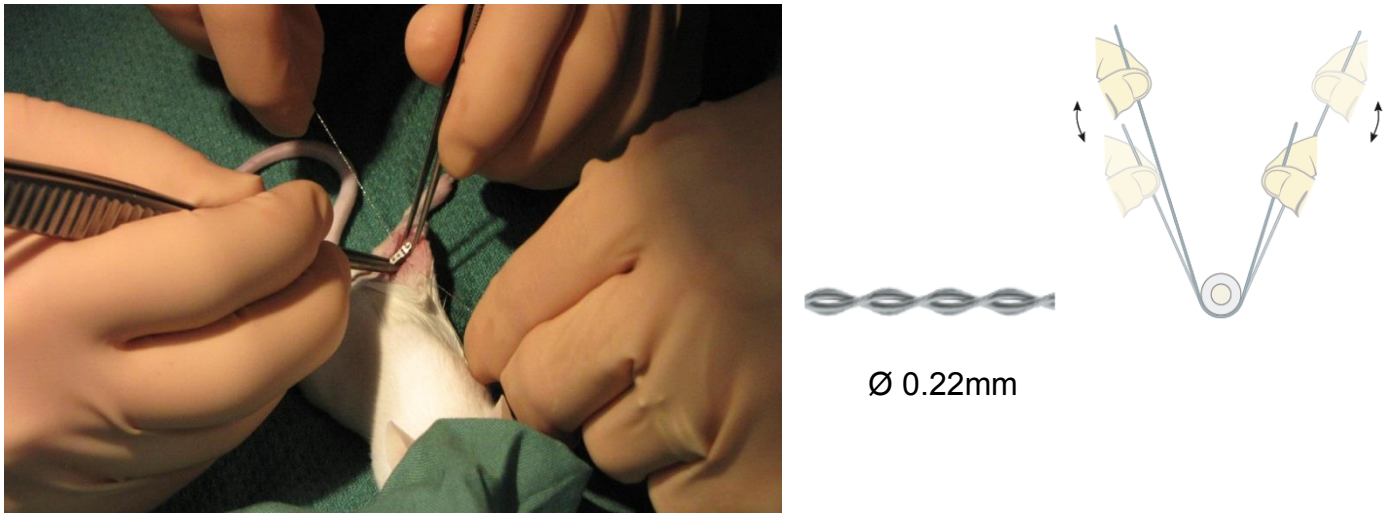

Fig.18.Creation of the transverse osteotomy with a Gigli saw
(photo from author's archive, images adapted from RISystem™, Davos, Switzerland (RISystem 2009))
URL: http://www.risystem.com/Standardized_Implant_for_Research/MouseFix.html accessed Jun 10, 2013)

According to the study protocol, mice were euthanised at 14 and 28 days byCO_2 asphyxiation, according to the NHMRC guidelines ((NHMRC) 2008). Individual animals were placed in the closed chamber, which was slowly filled with CO_2, and remained there until expiration (approximately 3-5 mins) (**Fig. 19**).

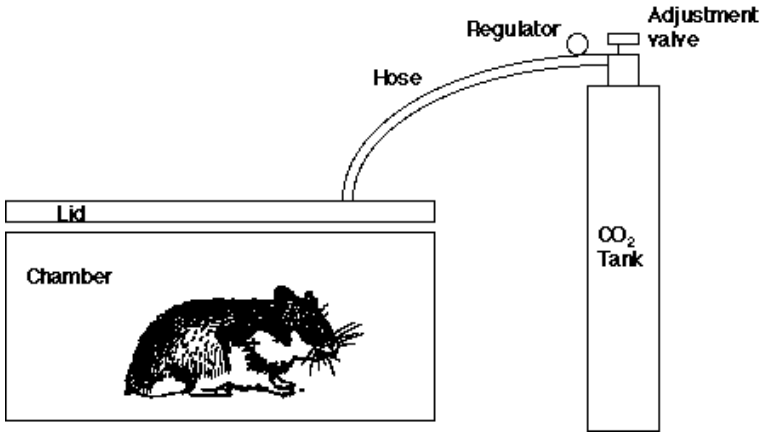

Fig. 19. Sacrifice by CO2 asphyxiation(Minnesota 2009)
(URL: http://www.ahc.umn.edu/rar/euthanasia.htmlaccessed Jun 11, 2013**)**

Death was confirmed by absence of heartbeat and blinking reflex or, if these findings were equivocal, by surgical pneumothorax. After euthanasia, mouse femora were explanted by disarticulation and cleared of soft tissue with

preservation of callus. They were then wrapped in gauze and soaked in Phosphate Buffered Saline (PBS) solution and stored at -20°C until mechanical testing.

7.3. Mechanical testing

For the evaluation of the mechanical integrity of the healing bones, in order to assess the progression towards recovery of the original properties, we used 3-point bending stiffness measurements. This test measures the ability of the bone to resist deformation under load, and provides values for the modulus of elasticity and, if done to failure, the flexural strength of the bone (**Fig. 20**) (Bird and Ross 2012). In this experiment, the stabilizing implant was removed prior to testing, the bone was horizontally fixed in a universal testing machine, and a known load was applied to the bone on its free end. The same set up was used to test all the specimens. An important point to mention is that the results of this type of three point bend test are not directly comparable with those of a simply supported three point bend test, because the applied force is not shared equally between the two supports.

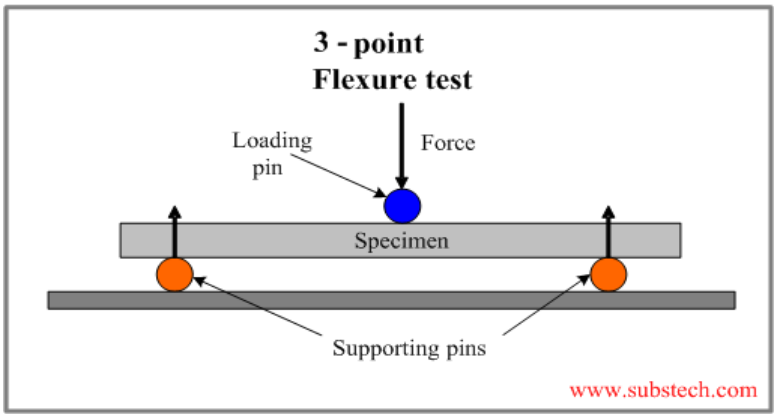

Fig. 20. Three-point flexural stiffness test(adapted from "Substances and Technologies"(Kopeliovich 2012))
(URL:http://www.substech.com/dokuwiki/doku.php?id=flexural_strength_tests_of_ceramicsaccessed Sep 10, 2013)

In contrast to other methods of assessment of fracture healing (radiology or manual examination), it is quantifiable and objective (Claes and Cunningham 2009), and is a preferred mechanical testing method for determining mechanical properties of murine bones

Prior to mechanical testing, femur pairs were thawed in groups of four to be tested on the same day. Once the bones were at room temperature, excess soft tissue was removed and fixation plates and screws removed from the right femora. The exclusion criteria for proceeding with the testing were gross deformity at the fracture site, malalignment of the fractured ends, movement of bone fragments under the plate, massive callus (indicating fixation failure), and loosening of the plate on the bone. We had no fixed criteria when to exclude bones from the analysis, but if a visible deformation or malalignment was seen, the samples were excluded as they could not be used for mechanical testing.

Similarly, there was no specific callus volume cut-off used. The decision to exclude specimens from the study was made on a case-by-case basis at the time

of mechanical testing, where based on unusually large or deformed calluses some samples were deemed to be not suitable for testing. The pins were deemed loose if, on inspection, the threads of the screw heads were no longer engaged with the thread in the plate, or the screws were found to be loose in the bone due to bone resorption.

We used an “offset” three-point bending set-up in our experiment, with the centre load applied at the metaphysis (**Fig. 21**).

Fig 21. Three-point bending test of a mouse femur(Claes et al. 2009)

The distal ends were clamped in the potting assistant and secured with PMMA in the aluminium insert. Before testing, images were taken from each femur in the setup, with a ruler imaged parallel to the bone (**Fig. 22**).

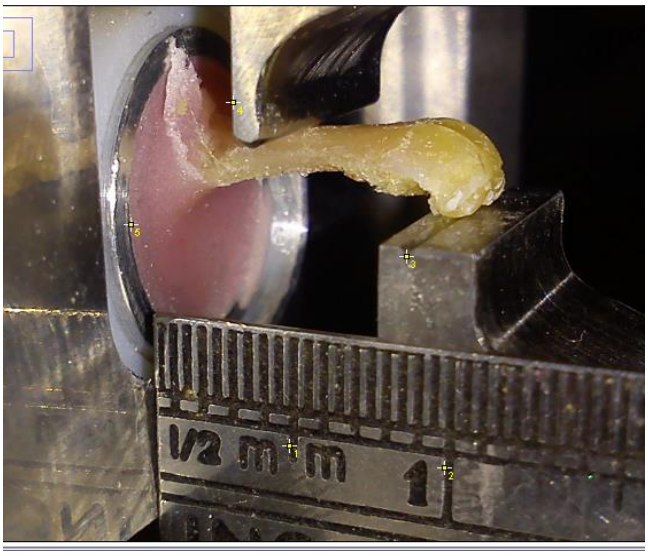

Fig. 22. Measuring the distance between the supports and the top point load

From these images, the exact distance between supports and the top point load was determined using digital image analysis methods. Each image was opened with Image J, an image processing and analysis program written in Java®(Abramoff, Magalhaes et al. 2004). Using the program, points were placed on the distal and proximal supports, the top point load and on the ruler. The measure function was utilised, resulting in a list of data containing the x and y coordinates in pixels of the five points. The conversion multiplier for pixel to millimeter was derived for each sample by subtracting the x-coordinate for point 1 from that of point 2, then dividing by 5 to find number of pixels per millimeter. The inverse of this forms the multiplier.

$$\frac{5}{x_2 - x_1} = multiplier\left(\frac{mm}{pixel}\right)$$

This multiplier was then used to convert the distances between points 3, 4 and 5 from x-coordinate pixels to millimeters.

The bones were then subjected to the 3-point bending stiffness test (Instron® 5848 Microtester, USA). This test measures the force required to bend a beam under 3-point loading conditions, with the flexural modulus used as a measure of a material's stiffness.

The left femur was tested first, followed by the right femur. Each bone was tested five times with a 0.1N preload to extension of 0.1mm over a 10 second duration. The load deformation data was recorded and saved in Excel (Excel® 2007). A combination of the modified MATLAB script(MATLAB® 7.10.0, The MathWorks Inc., 2010) and an Excel® template were used to calculate the **extrinsic stiffness (EI,** Nmm^2**)** of the bone. **Extrinsic** stiffness (**EI**), or flexural rigidity of the bone, varies with bone size, shape and quality of its constituents. The outcome parameters were calculated both in terms of absolute values (stiffness under load in N/mm), as well as in percentages for the fractured bone compared to the intact contralateral bone. EI is equal to the slope of the elastic region of the ***load-deformation*** curve (**Fig. 23**). In this experiment, the EI is approximately 45 N/mm.

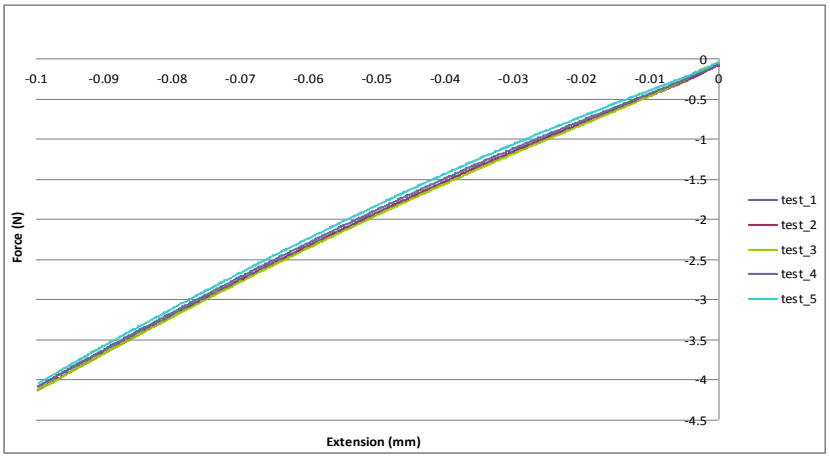

Fig. 23. Representative load-deformation curve(Mouse #13, 28 days timepoint, 65% stiff group) **indicating the linear nature of the curve and the reproducibility of stiffness measurements.**

7.4. MicroCT analysis of callus formation

Explanted bones were processed in the microCT scanner (Scanco µCT® 40, Brüttisellen, Switzerland) after mechanical testing. The samples were scanned at an voltage of 55 kV and an current of 145 µA In CT imaging, **attenuation** refers to the extent to which the x-rays are absorbed by the tissue**.** Dense tissue, such as compact cortical bone, will absorb most of the radiation, and on the CT image will appear stark white with sharp, defined edges, and will have a high HU value. In contrast, bony callus will appear diffusely grey with soft edges due to its loose organisation and low attenuation of the x-ray beam, and will have a low HU value.

The reconstructed scans were evaluated using the scanner's software (Scanco®µCT Evaluation Program, V6.5-1, Scanco Medical, Bassersdorf, Switzerland).In order to calculate the V_{call}, it was necessary to first determine the entire bone volume (ie cortical bone volume + callus volume) and the cortical

bone volume. To achieve this, the reconstructed microCT data underwent segmentation. Briefly, an irregular manual contour around the bone was manually drawn around the first two slices, a few pixels away from the edges of the visible callus. The region of interest **(ROI)** included the area between the edges of the proximal and distal screws on either side of the osteotomy. The contoured region included the bone (cortical and cancellous) and any visible (i.e. partially mineralised) callus. The program would then find the edge of the callus automatically for all subsequent scans. Further adjustments were made manually when necessary, if the automatic contour was found inaccurate. The data was analysed, and the number of the pixels in contoured regions were summed and converted into the volumetric units (mm^3). Finally, the total bone volume was calculated as the sum of the total bone volumes in individual slices.

After contouring, thresholding of the total callus volume was done in order to determine the (mineralised) callus volume. Thresholding involved repeating the contouring process within a different greyscale range. Threshold was chosen visually to best represent the cortical bone and mineralised callus compartment based on a few sample scans, and then kept constant for all evaluations. Voxel size was 12 microns. Bones were scanned without implants, so no metal artefact reduction was necessary. The first range of greyscale values was wide (312 – 1994.7 mgHA/cm^3) and included both the bright white cortical bone and a grey, diffuse callus tissue, the second time the greyscale range was narrower (873 – 1994.7mgHA/cm^3), and included only the cortical bone. In the first analysis, the derived volume represented the sum of cortical and callus volume of the region,

and in the second analysis, the volume included only the cortical bone. The difference between these two values provided the callus volume of the contoured region.

$$V_{Callus} = V_{Total} - V_{Cortical\ bone}$$

A Gaussian filter with sigma = 0.8 and support =1.0 was used to remove the noise from the reconstructed images.

7.5. Histologic and histomorphometric analysis

Three fractured tibiae from each group were selected for histological characterization of the callus region after biomechanical testing and microCT analysis. The tibiae were fixed in 10% neutral buffered formalin (NBF) for 2 days. NBF is a general-purpose fixative, suitable for most biological tissues, which permits the use of most staining techniques(An and Martin 2003). This was followed by decalcification in ethylene diaminetetraacetic acid (EDTA). The aim of decalcification of bone tissue is to produce a sample of homogeneous consistency for embedding in paraffin by reducing the original tissue density. The progress of decalcification was monitored by serial microCT scans. After decalcification, the water in the tissue was removed by successive bathing of the specimens in increasing concentrations of ethanol followed by immersion in xylene (a lipid solvent) to remove the alcohol. Decalcified bones were embedded in paraffin (Paraplast® Highmelt Paraffin, Leica Biosystems).

Longitudinal sections in a sagittal plane in its primary bending plane were cut at 5 µm by a microtome (Leica® SM 2265, Germany). The stains used were Safranin O/Fast Green and Haematoxylin and Eosin (H&E). Safranin-O binds to the proteoglycans present in the cartilage tissues, colouring them orange. Fast green, the contrast stain of Safranin-O, binds strongly to the amino groups on protein and thereby strongly stains the non-collagen sites (An and Martin 2003). Cartilage was identified by the orange colour of the Safranin O stain in these sections. The stained histological slides were scanned at a magnification of 20x with a slide scanner (Leica® SCN400) and the images archived using SlidePath® Digital Image Hub software (Leica® Microsystems GmbH, Wetzlar, Germany). The slides then were visually inspected under the microscope for presence or absence of cartilage. Normally, cartilage is associated with the lining of articular surfaces and with the growth plate. However, cartilage is also one of the main constituents of the fracture callus in the endochondral ossification mode of healing (Cruess and Dumont 1975) and in this study we therefore used cartilage presence as a marker for endochondral ossification.

7.6. Statistical evaluation

All data are given as means +/- standard error of measurement. SPSS® (IBM SPSS Statistics 21.0, IBM Inc.) software has been used for statistical analysis. First, the Shapiro-Wilk test for normality has been used on each outcome variable to prove the normal distribution. Subsequently, analysis of

variance (ANOVA) has been used to determine the difference between treatment groups on each variable, and the student t-test was used to test the differences between the individual groups. The assumptions of the ANOVA model are that the observations are independent, the residuals are normally distributed and the variance is the same between groups. A p-value of <0.05 was considered to indicate significant differences between the groups.

8. RESULTS

8.1. Gross observation

Surgeries for application of fracture fixation plates of three different stiffnesses to the osteotomised femora were conducted on 63 animals. Early sacrifice due to complications was necessary in four animals. The causes for these complications were different in each animal. One animal developed a severe limp with the operated leg, indicating a fixation failure, which was confirmed at the post-mortem evaluation. An intra-operative fracture and consequent fixation failure occurred in another animal. A third animal suffered from post-operative seizures which could be explained by an allergic reaction to the anaesthetic gases. Finally, a fourth animal was euthanized due to a severe infection of the surgical wound. The remaining animals stayed healthy, with ambulatory function returning to normal within hours of the operation. Upon initial examination during extraction, all bones were healed. Where re-fracture was suggested by malalignment of the fracture fragments, an abnormally large

callus, movement of the bone fragments under the plate, a massive callus, or loosening of the plate pins, the specimens were excluded from further analysis. In total, 45 of 63 bone pairs were suitable for testing.The remaining bones were disqualified for placement of the plate in the wrong region on the bone (diaphysis), obvious re-fracture, visible pin loosening or breakage, or fracture of the bone during mechanical testing. The bones were grouped according to stiffness and sacrifice time point, for a total of six groups. For the 14-day timepoint, there were 9, 7 and 7 animals in 45%, 65% and 100% stiff groups, respectively. For the 28-day timepoint, there were 9, 5, and 7 animals in 45%, 65% and 100% stiff groups, respectively.

8.2. Mechanical testing

Of the 45 pairs suitable for testing, one bone broke during preparation for testing. The %EI was calculated for all six groups. At 14 days after fracture, the relative stiffness of the healing bones compared to the contralateral, unfractured bone at the fracture site showed a trend towards highest values in the bones stabilised with a 45% stiff plate (30.6 +/- 6.5), followed by the bones stabilized with a 100% stiff (25.5 +/- 10.6) and 65% stiff (18.2 +/- 5.4) plates (**Fig. 24** and **Table 4**). However, these differences were not statistically significant ($p = .528$).

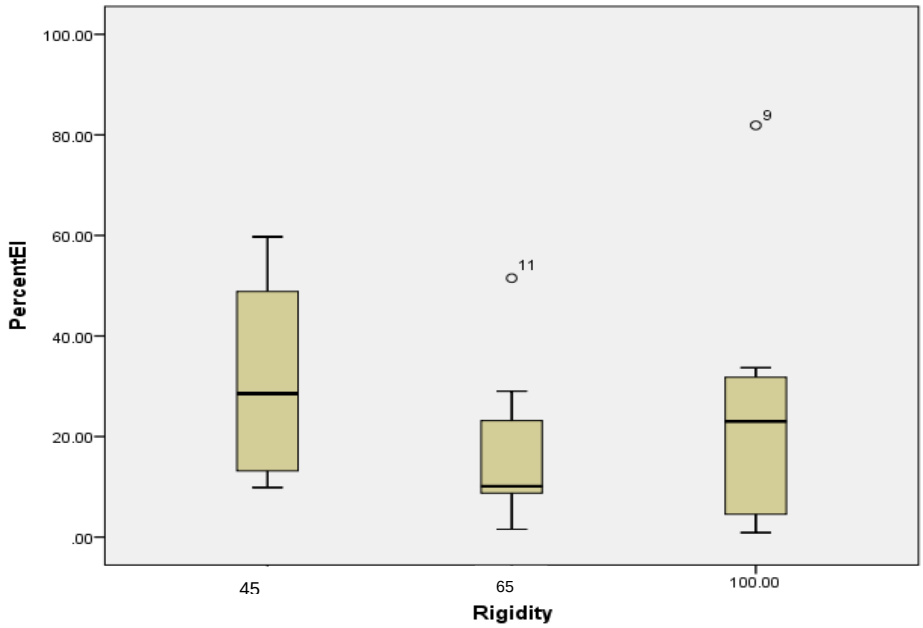

Fig. 24. %Extrinsic Stiffness (%EI) at 14-day time point relative to contralateral side

	100% stiff (n = 7)	**65% stiff** (n = 7)	**45% stiff** (n = 9)	**p-value**
%Extrinsic Stiffness (%EI)	25.5 +/- 10.6	18.2 +/- 5.4	30.6 +/- 6.5	.528

Table 3. Change in %Extrinsic Stiffness (%EI), N/mm, at 14 day time point

When the three groups were tested for variation between individual groups, and the outliers were excluded, there was a statistically significant difference in %EI between the 45% stiff and 65% stiff groups with p = 0.011 (p = 0.095 with outliers included).

At 14 days:

	p-value	P-value (outliers excluded)
45% vs 65%	0.095	0.011
45% vs 100%	0.338	0.271
65% vs 100%	0.284	0.143

At 28 days after fracture, for the percent stiffness a trend towards highest values in the bones stabilized with the 65% stiff plate (76.1 +/- 9.5), less in the bones fixed with the 45% stiff plate (60.7 +/- 15.6), and least in the 100% stiff bones (45.6 +/- 8.8) (**Fig. 25** and **Table 5**) could be observed. However, the differences between these three groups were also not statistically significant (p = .354).

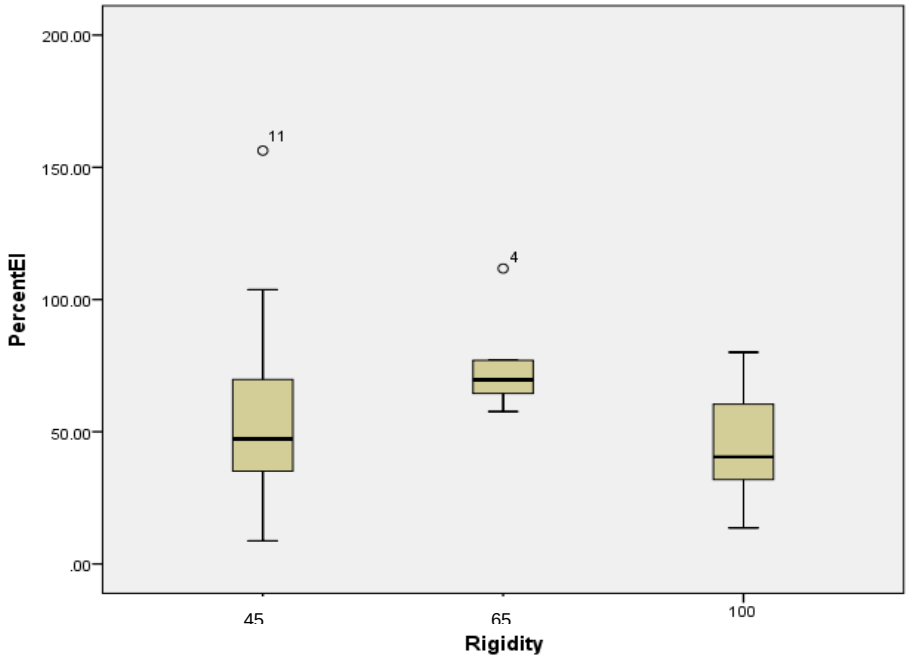

Fig. 25. %Extrinsic Stiffness (%EI), at 28-day time point, relative to contralateral side

	100% stiff (n = 7)	**65% stiff** (n = 5)	**45% stiff** (n = 9)	**p-value**
%Extrinsic Stiffness (%EI)	45.6 +/- 8.8	76.1+/- 9.5	60.7 +/- 15.6	.354

Table 4.Change in %Extrinsic Stiffness (%EI), N/mm, at 28-day time point

When the three groups were tested for variation between individual groups, the only statistically significant difference in %EI was between the 65% stiff and 100% stiff groups with p = 0.021.

At 28 days

	p-value
45% vs 65%	0.206
45% vs 100%	0.207
65% vs 100%	0.021

As expected, %EI at 28 days was higher than %EI at 14 days. For the 45% stiff implants, the change in stiffness was marginally significant ($p<0.1$), while it was not significant for the 100% stiff plate group (p = .171, respectively). The change in %EI was greatest in the 65% stiff group, from (mean) 18.2 to 76.1, with $p < .001$ (**Table 26 and Fig. 6**).

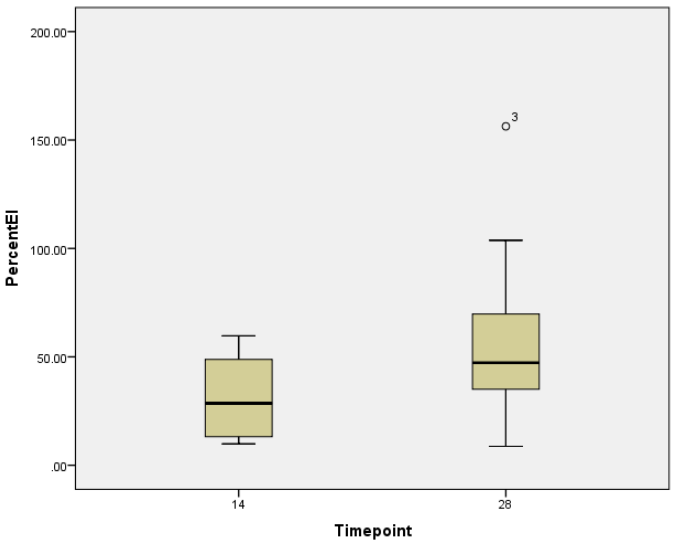

a)

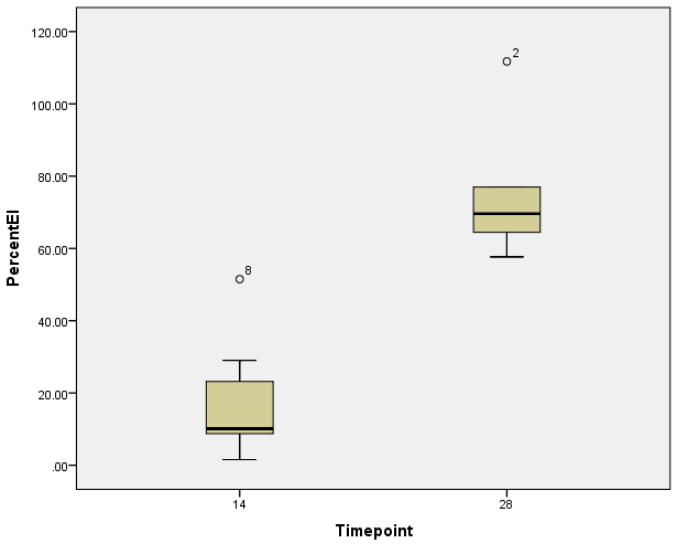

b)

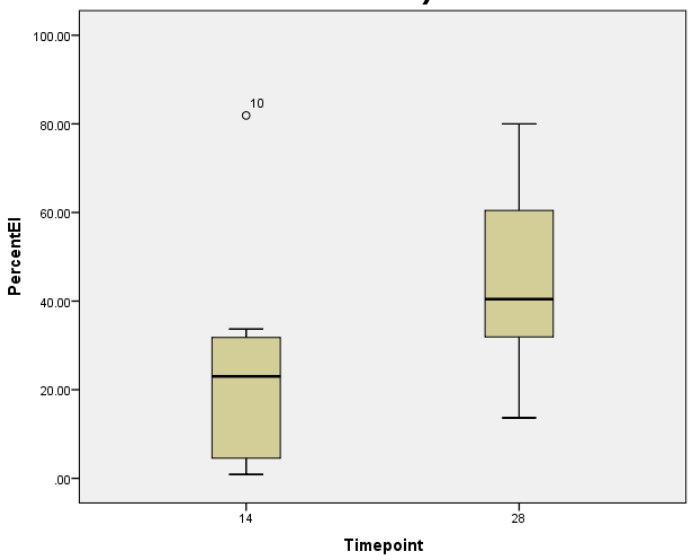

c)

Fig. 26. Change in %EI between 14 and 28 days in a) 45% stiff b) 65%stiff and c) 100% stiff groups

% Extrinsic Stiffness (%EI)	14 days	28 days	p-value
45% stiff	30.6 +/- 6.5	60.7 +/- 15.6	p<0.1
65% stiff	18.2 +/- 5.4	76.1 +/- 9.5	p<.001
100% stiff	25.5 +/- 10.6	45.6 +/- 8.8	p=0.171

Table 5. Change in %Extrinsic Stiffness between two timepoints

8.3. MicroCT

In this study, the evaluation of the microCT scans demonstrated a similar proportion of total callus volume in all three groups at 14 and at 28 days after the fracture, reflecting the same amount of callus in all groups, regardless of fixation rigidity.

At 14 days, the microCT results showed a similar distribution of total callus volume, with no significant differences between the three groups. (**Fig. 27 and Table 7**). These findings support the results of mechanical testing, which showed no significant differences in callus stiffness among the three groups.

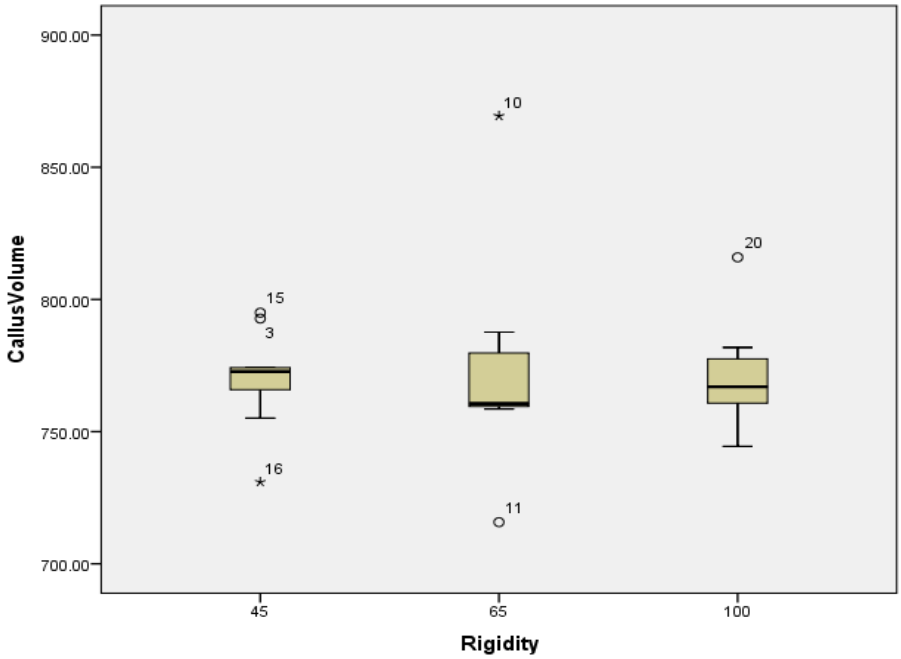

Fig. 27. Callus Volume (V_{call}) at 14-day time point

	100% stiff (n = 7)	**65% stiff** (n = 7)	**45% stiff** (n = 9)	**p-value**
Callus Volume (V_{call}), mm^3	772.0 +/- 8.4	769.8 +/- 6.5	774.9 +/- 17.8	.948

Table 6.Callus Volume (V_{call}) at 14-day time point

At 28 days, the callus volume (V_{call}) was slightly increased in all three groups (although only significantly in the 45% stiff group), with the variance of the values increasing, resulting in the differences between the groups not being statistically significant (p = .176) (**Fig. 28** and **Table 8**). V_{call} appeared greatest in the 65% stiff group at this time point, supporting the results of the mechanical testing, where the %EI was also highest in the 65% stiff group at this stage of healing.

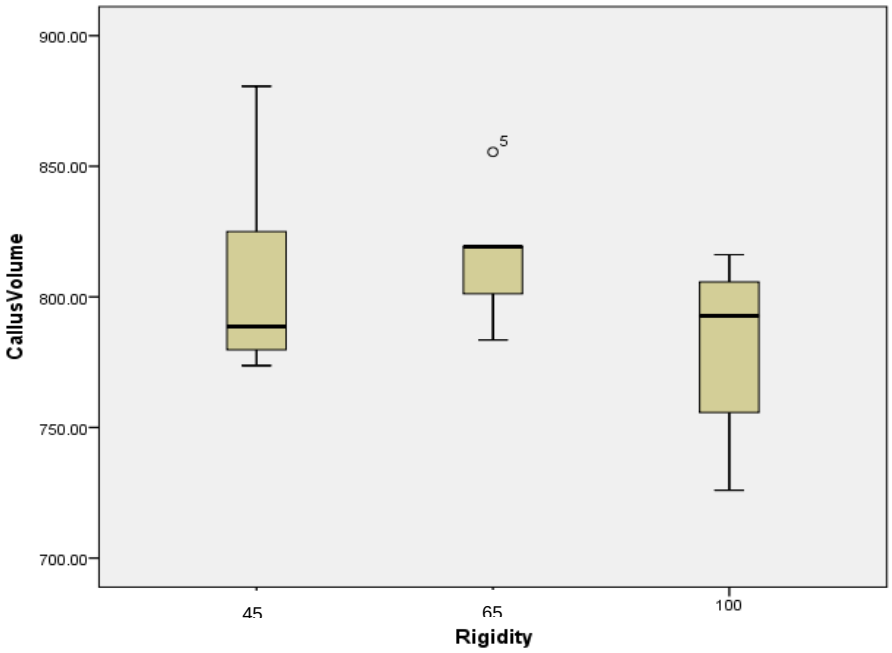

Fig. 28. Callus Volume (V_{call}) at 28-day time point

	100% (n = 7)	**65%** (n = 5)	**45%** (n = 9)	**p-value**
Callus Volume (V_{call}), mm^3	808.9 +/- 13.1	815.2 +/- 15.4	789.7 +/- 11.3	.176

Table 7.Callus Volume (V_{call}) at 28-day time point

The amount of total callus, formed around the fracture, increases as healing progresses, reflected by a higher total callus volume present in all three groups at 28 days than there was at 14 days (**Table 9 and Fig. 29**).

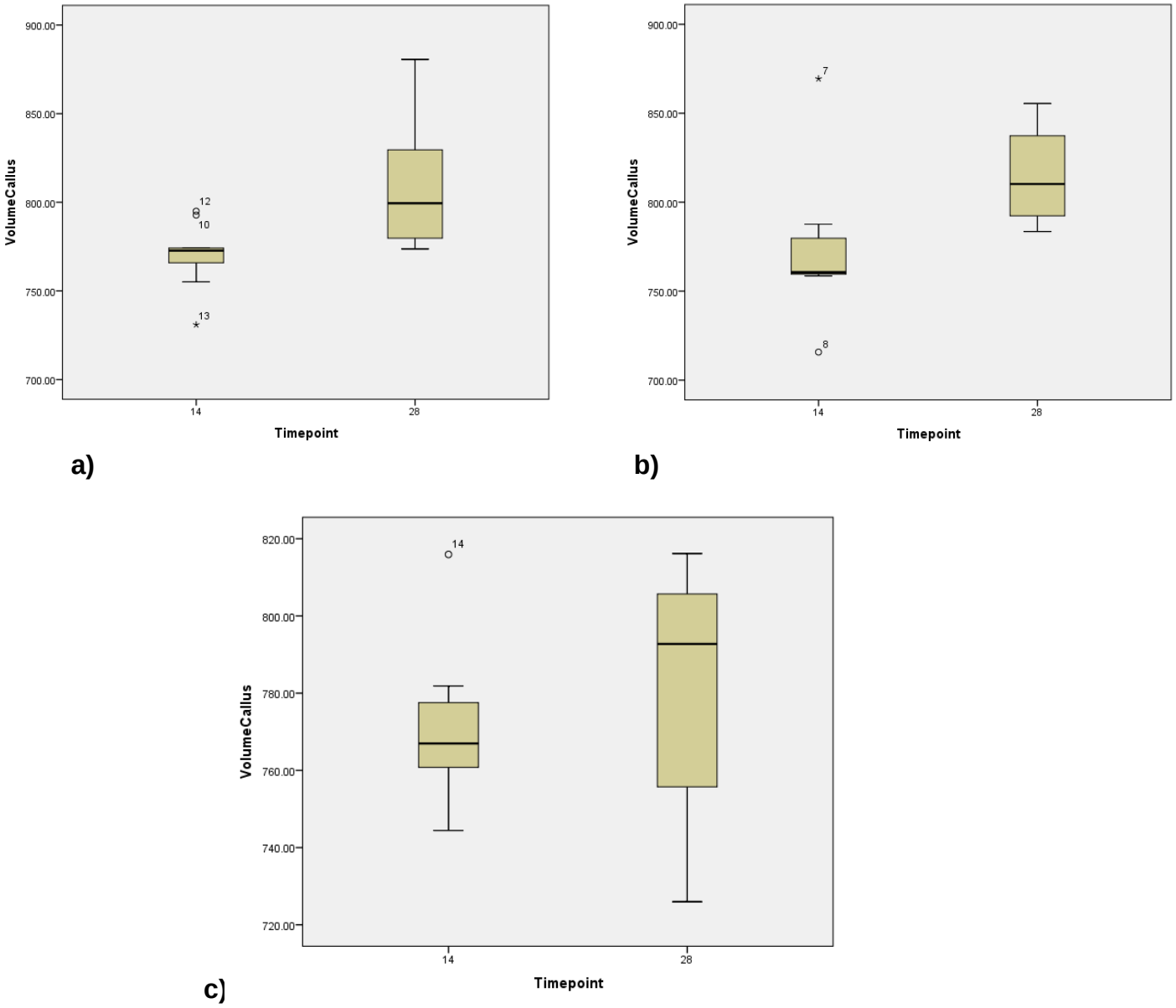

Fig. 29. Change in callus volume between 14 and 28 days in a) 45% stiff, b) 65% stiff, and c) 100% stiff groups

Callus Volume (V_{call}), mm^3	14 days	28 days	p-value
45% stiff	774.9 +/- 17.8	781.3 +/- 11.3	.017
65% stiff	769.8 +/- 6.5	814.9 +/- 15.4	.166
100% stiff	772.0 +/- 8.4	808.9 +/- 13.1	.534

Table 8. Mean callus volume (V_{call}) at 14-day and at 28-day time points in all groups

There was no significant difference in callus volume between the individual groups at both timepoints.

14 days

	p-value
45% vs 65%	0.194
45% vs 100%	0.420
65% vs 100%	0.227

28 days

	p-value
45% vs 65%	0.208
45% vs 100%	0.290
65% vs 100%	0.291

8.4. Histologic and histomorphometric analysis

Three fractured tibiae from each group were selected for histological analysis. The stains used were Safranin O/Fast Green (SafO) and Haematoxylin and Eosin (H&E). The results of the analysis are summarized below:

- 45% stiff group: at 14 days, there is abundant cartilage demonstrated in the vicinity of the osteotomy in two out of three examined femurs (2/3), indicating endochondral ossification. The fracture ends are not united at the cortical edges, but the osteotomy site is filled with woven bone, which signifies intramembranous ossification. At 28 days, there was no cartilage observed in any of the specimens (0/3). The fracture ends are united and in good alignment, but there is still a defect in cortical bone on both side of the osteotomy, indicating a lag in cortical bone repair as compared to cancellous bone.

- 65% stiff group: cartilage was observed in one out of three (1/3) slides at both 14 and 28 days mark. The cartilage is not as abundant as it is in the 45% stiff group at 14 days mark. However, there is more prominent woven bone formation in and around the fracture gap. The alignment of the fracture ends is preserved.
- 100% stiff group: there was no visible cartilage (0/3) at 14 days, and there was cartilage noted in one out of three slides (1/3) at 28 days (**Table 10 and Fig. 30-32**). However, there is vigorous woven bone formation in the osteotomy gap at both 14 and 28 days, stabilising the fracture site and maintaining the alignment of the fracture ends.

Stiffness	14 days	28 days
45%	2/3	0/3
65%	1/3	1/3
100%	0/3	1/3

Table 9. Counts of cartilage occurrence in callus tissue

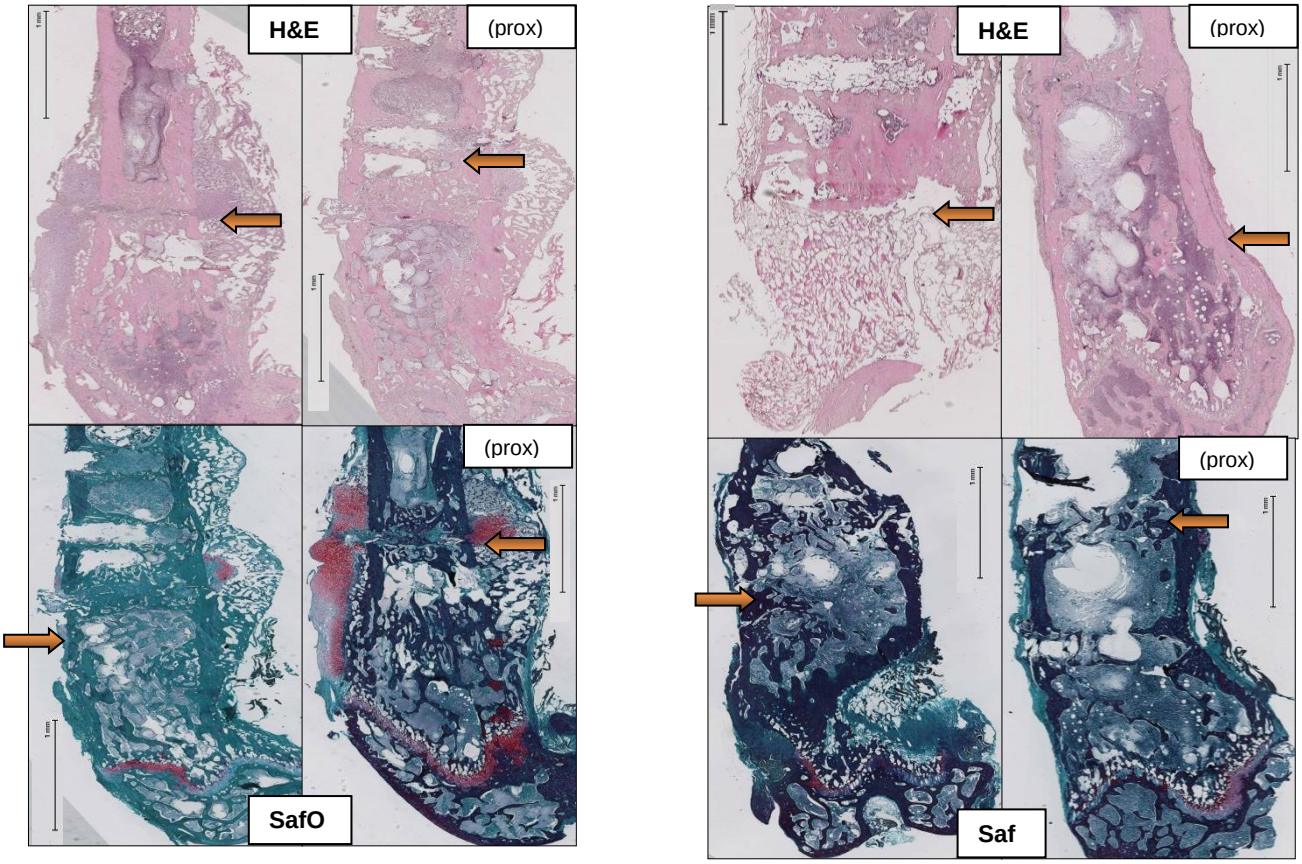

a) b)

Fig. 30. Histological appearance of 45% stiff group at a) 14 days and b) 28 days (osteotomy site indicated with an ⇒)

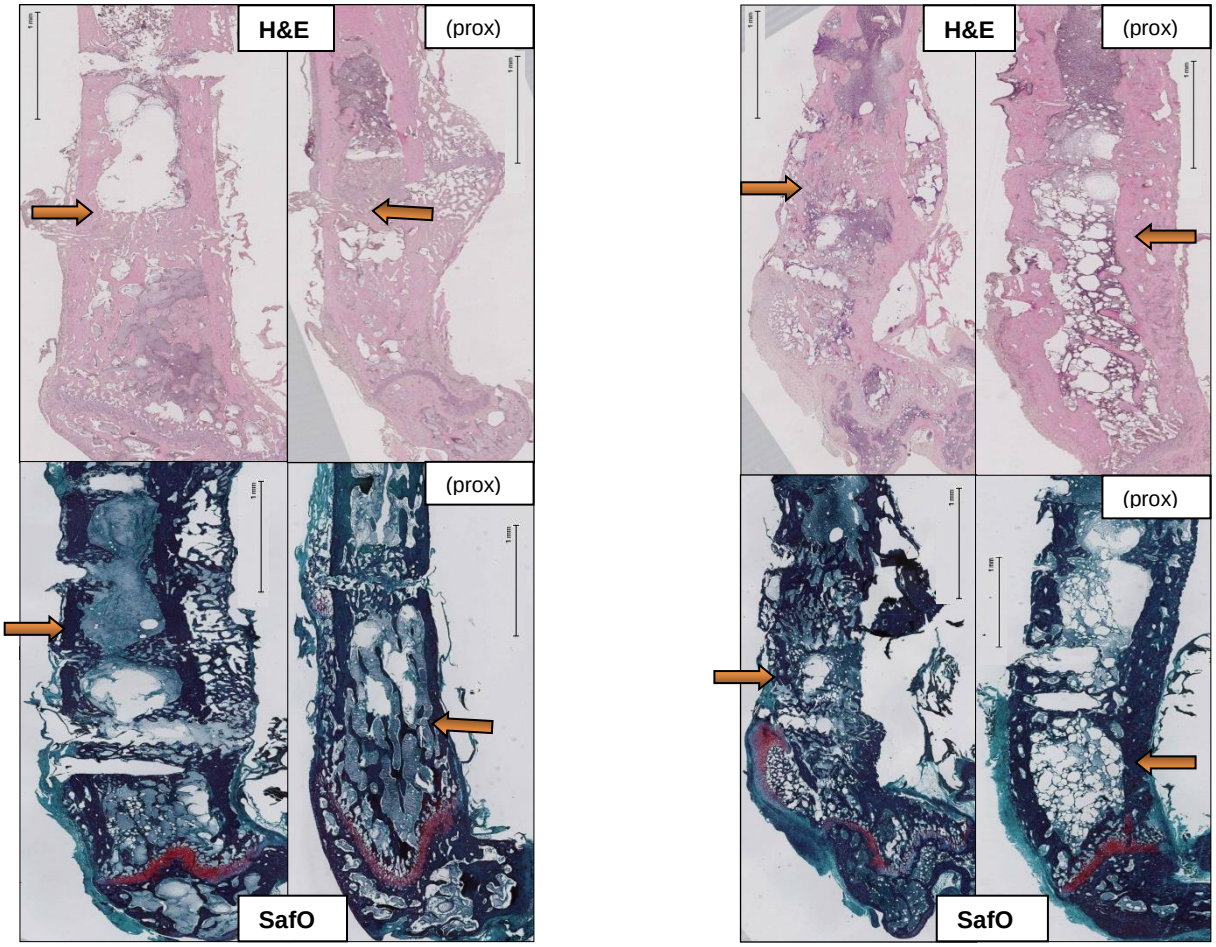

a) b)

Fig. 31.Histological appearance of 65% stiff group at a) 14 days and b) 28 days(osteotomy site indicated with an ⟹)

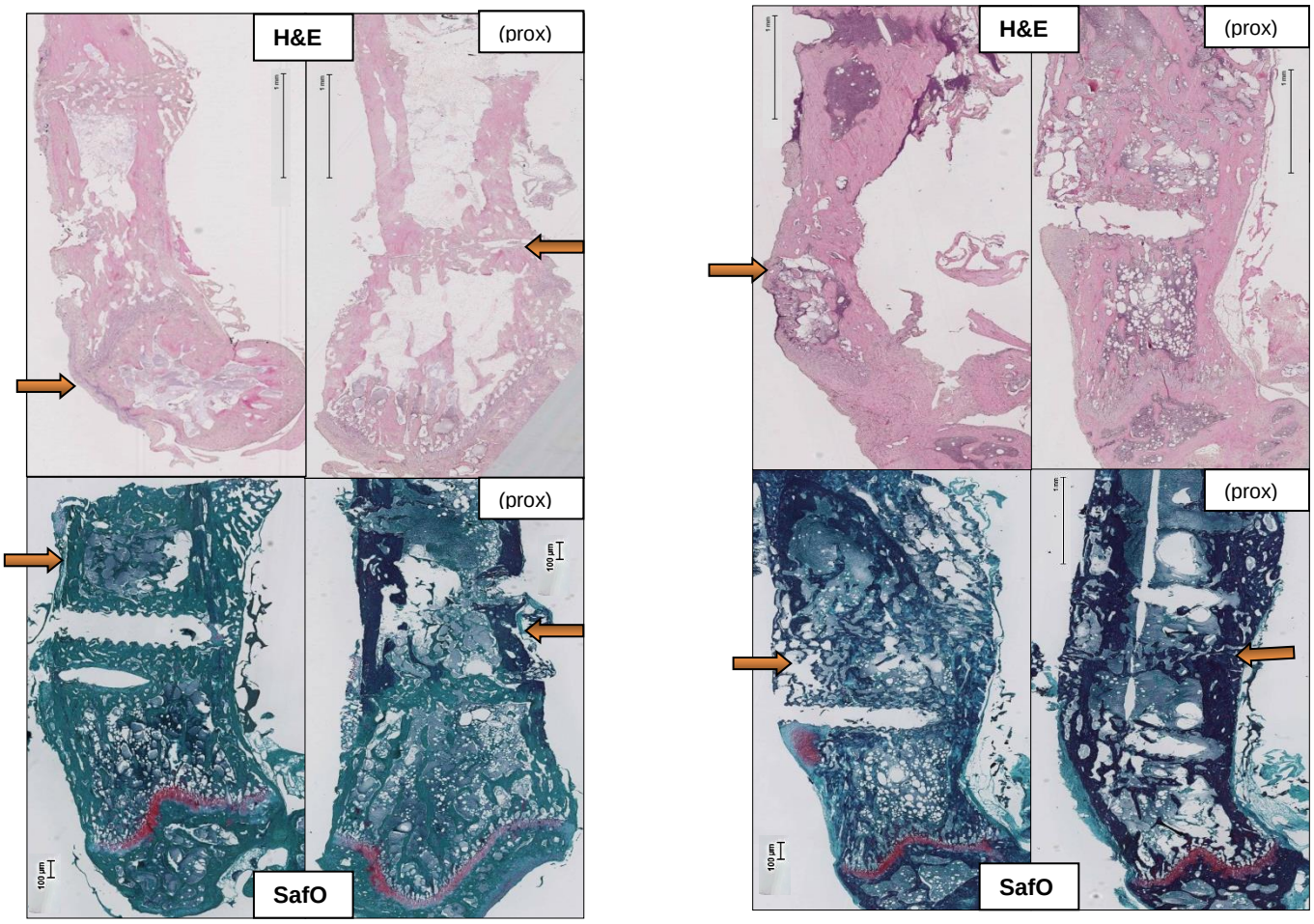

a) **b)**

Fig 32.Histological appearance of 100% stiff group at a) 14 days and b) 28 days

A summary of all results is provided in following overview figure:

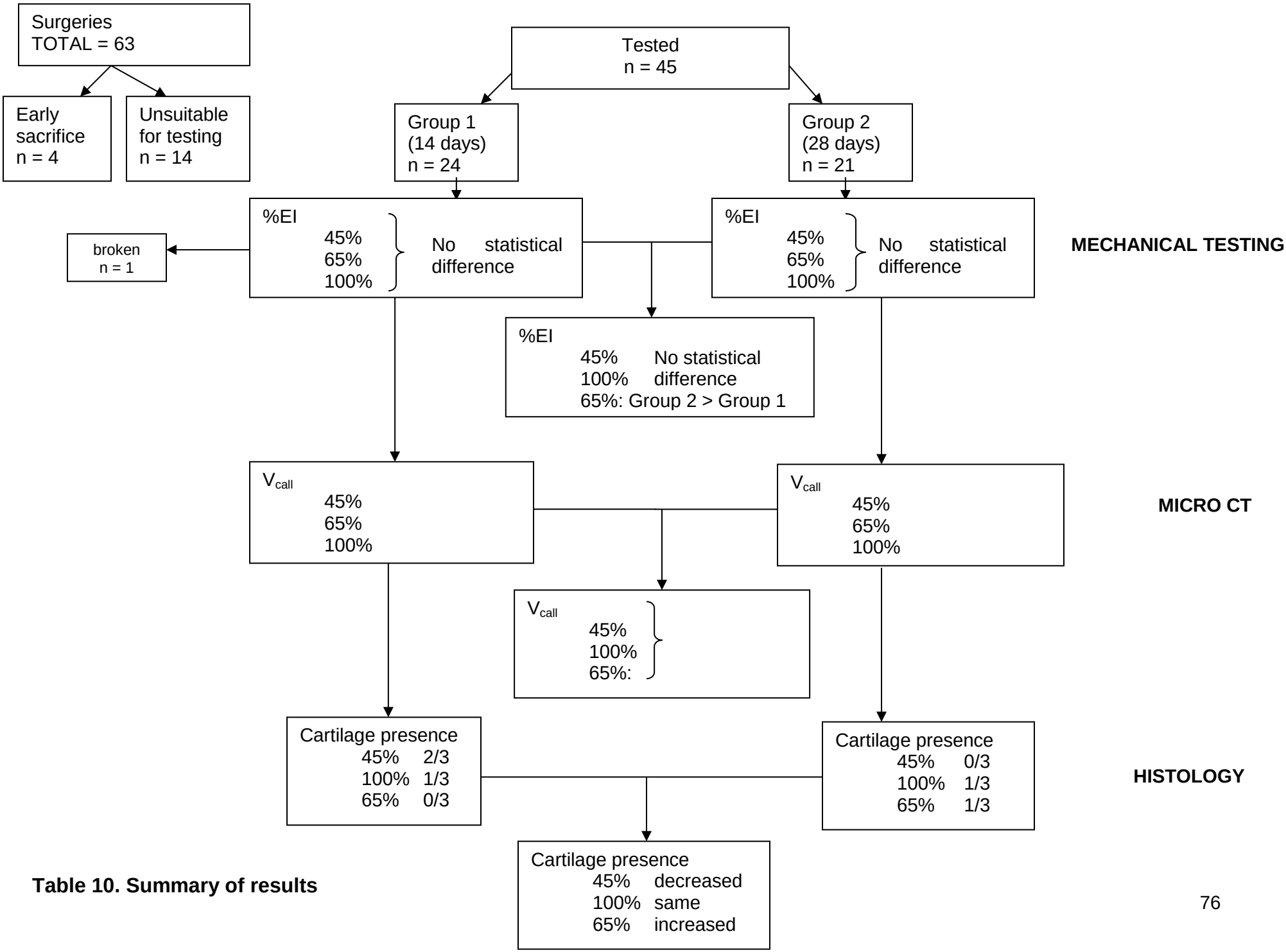

Table 10. Summary of results

9. DISCUSSION

In this study, we used an experimental model of a distal femur osteotomy, stabilized by plates with varying bending stiffness and fixed to the bone fragments using locking screws, to investigate the influence of the mechanical conditions on the healing of fractures in the metaphyseal bone of the distal femur in mice. Our main goal was to test the hypothesis, whether the fixation stiffness affects the healing of metaphyseal bone fractures similarly as it does in the healing of diaphyseal bone fractures. To achieve this, we aimed to answer the following questions:

1. Does the implant stiffness affect the bone repair mechanism in metaphyseal bone fracture healing; i.e. are stiff implants leading to predominantly intramembranous ossification and more flexible implants leading to mainly endochondral ossification?
2. Is the amount of callus formed directly related to the flexibility of internal fixation?
3. Is the bending stiffness of the healing bones dependent on the flexibility of the internal fixation?

To answer our first question, concerning the influence of fixation stiffness on the predominant mode of ossification of metaphyseal bone after the fracture and to compare it to diaphyseal bone healing, we used histological evaluation. Stained histological slides were evaluated for gross morphology, and for presence or absence of cartilaginous tissue, which would indicate endochondral ossification pathways. At 14 days, all evaluated slides in the group of highest flexibility (45% stiff) showed evidence of cartilage, whereas only 1/3 in the 65% stiff group, and none in

100% stiff group. However, at 28 days, cartilage was not detected in any of the slides from the 45% stiff group, whereas 1/3 slides in the 65% and 100% stiff groups showed some presence of cartilage. In sum, we therefore found collagen in samples from all stiffnesses, indicating a mixture of endochondral and intramembranous ossification occurring in all three groups.

To answer our second question, we used microCT analysis to measure the **callus volume (V_{call})**, and to examine the pattern of callus formation in the groups of different fixation flexibility. In this study, V_{call} appeared to be very similar in all three groups, regardless of fixation stiffness.

The third objective of this study was to determine the relationship between the fixation stability and resultant bending stiffness of the healing bones. To answer this question, we used 3-point-bending test to determine the **extrinsic stiffness** (**EI**) of the fractured bones at the two time-points, and expressed it as a percent stiffness of the contralateral, unfractured femur (%EI).

While trends could be observed from the results of the mechanical testing, indicating highest bending stiffness (%EI) for the 45% stiff group at 14 days and for the 65% stiff group at 28 days, differences were statistically not significant

In summary, based on these results we can therefore not conclusively confirm or refute our main hypothesis for this study. While the histological results at 14 days showed a higher incidence of cartilage with increasing flexibility of fixation, at 28 days, the incidence of cartilage does not correlate with fixation flexibility anymore. The results of the histological evaluation are neither supported nor refuted by the microCT results, which did not detect any difference in callus volume between the different experimental groups. Based on the results of past research (**Table 1**, “Introduction”), we expected to observe some variability in the callus distribution in

our current study, with the greatest callus volume to be present in the 45% stiff population, and the least in the 100% stiff group. However, here the callus volume appeared to be very similar for all three groups, regardless of the time point and of stability of the fractured ends (**Table 9**). At the 14-day time-point, the average V_{call} seemed to be very similar in all three groups of different fixation stiffness (**Fig. 27** and **Table 7**). At 28 days, V_{call} appeared to have increased in all three groups, with a trend towards highest callus volume in the 65% stiff group, but the differences between the groups remained statistically not significant (**Fig. 28** and **Table 8**).

Likewise, the mechanical testing results neither supported nor refuted the findings from the histological evaluation. Similar to the microCT findings, the mechanical testing results were inconclusive, demonstrating no significant differences between the groups, both at the 14-day and 28-day mark (**Fig. 26** and **Table 6**). As expected, both %EI and V_{call} showed a trend towards higher values at 28 days than at 14 days, reflecting the progress of healing. However, the only statistically significant changes was the increase in V_{call} of the 45% stiff group ($p = .017$) and %EI change in 65% stiff group ($p < .001$) between 14 and 28 days.

Previous studies, examining the relationship between the fixation stability and callus formation, have shown that in diaphyseal bone the volume of callus formed is directly related to the flexibility of the stabilising implant and the amount of interfragmentary movement (IFM) at the fracture site. As suggested by Perren's interfragmentary strain hypothesis, the stimulating factors for callus formation are the IFM and the gap between the fracture ends (Perren and Cordey 1980).The interfragmentary strain for ultimate fracture healing lies somewhere between 5 and 20%, where the amount of IFM is sufficient to stimulate endochondral ossification and the formation of a callus, yet the amount of movement is small enough to also

achieve bony union. A stable mechanical environment, achieved with rigid fixation, will result in interfragmentary strain of <5%, and will heal via intramembranous ossification with no callus. So far, research on the healing mechanism of metaphyseal fractures is inconclusive.

Early experiments by Jarry and Uhthoff (Jarry and Uhthoff 1971, Uhthoff and Rahn 1981) investigated metaphyseal healing under stable and unstable conditions in different species. Their findings demonstrated that there was no callus forming under stable conditions, but that there was evidence of endochondral ossification with callus formation under unstable conditions. Uusitalo et al (Uusitalo, Rantakokko et al. 2001) studied the healing of the bony defect in the metaphyseal region of a mouse, and found that it healed by a combination of endochondral and intramembranous ossification. Han et al(Han, Zhang et al. 2012) found that the metaphyseal fracture in rabbits healed by solely by intramembranous ossification under stable conditions. However, a shortcoming of all these studies was that the biomechanical conditions were not very well defined. Later experiments on larger animals, such as sheep, by Claes et al (Claes and Cunningham 2009, Claes, Reusch et al. 2011), suggested that metaphyseal fractures healing follows the same path as the healing of diaphyseal fractures. In these studies, researchers attempted to regulate the biomechanical environment, and found that the IFS <5% delaying healing, and IFS between 5 and 20% resulting in a more pronounced bone formation by a combination of intramembranous and endochondral ossification. Later studies by Histing et al confirmed that rigidly fixed fractures heal primarily through intramembranous ossification(Histing, Klein et al. 2012). In the current study, the results of the microCTanalysis are inconclusive, with the Vcall unchanged between the groups, regardless of fixation flexibility. Also, in this study, all groups had both

cartilaginous tissue and woven bone present at the fracture site at the early healing stage, indicative of both endochondral and intramembranous ossification occurring simultaneously in all groups. Therefore, in this study, all three groups seemed to heal through a combination of the two bone healing processes.

Small animal models have been gaining popularity in medical research. particularly after decoding of the mouse genome and the possibility for genetic manipulation, which allows to create “custom-made” mouse models for studying of specific diseases, such as osteoporosis (Bostrom 1998).Fracture healing has also been addressed with mouse models, however, interpretation of the results have been hampered by the lack of a model which allows studying of fracture healing under highly defined, reproducible conditions(Jarry and Uhthoff 1971, Uhthoff and Rahn 1981, Uusitalo, Rantakokko et al. 2001, Han, Zhang et al. 2012). The original MouseFix® model allowed, for the first time, to define the biomechanical conditions in diaphyseal bone fracture healing by providing a choice of flexibility of fixation and of osteotomy sizes (Matthys and Perren 2009).The Trauma Research Group of QUT was involved in the characterization of the MouseFix® implants(Histing, Klein et al. 2012). The next development in a collaboration between RISystem and Trauma Research Group was focusing application of Mousefix® implants on studying of metaphyseal fracture healing. The main motivation for this study was to study the healing of metaphyseal bone under highly standardized, reproducible biomechanical conditions by application of existing MouseFix® implant to metaphyseal region of a mouse femur. Wereport application of MouseFix® implants to 63 animals. Three animals had to be euthanized prematurely due to complications arising during healing time. This represents a complication rate of 1.8%, which is below the recommended maximal value (5%) (Histing, Garcia et al. 2011), and a premature

sacrifice rate of 5.8%. However, after sacrifice and explantation of the fractured, healing limbs, a further 15 animals had to be excluded from further evaluation due to instability of the fracture or gross deformations. In sum, with a failure rate of over 28%, the criteria for standardized and reproducible biomechanical environment were not fulfilled in this study. Significant challenges were faced by using the MouseFix® implants in metaphyseal region of the bone, which are discussed in the following.

a) Small trabecular bone compartment in mouse bones: The main difficulty of this study was consistent fixation of the small murine bone with an even smaller plate.In this experiment, correct plate positioning meant that the distal end of the plate needed to be flush with the distal end of the bone, with the osteotomy located in the trabecular compartment of the metaphysis (**Fig 17**). However, it proved difficult to identify the correct region for plate position on the small mouse bone with a naked eye during surgery. If the plate was positioned as little as 1 mm off its optimal point, this resulted in placement of the osteotomy either too far distal (too close to the growth plate) or, in our experience more likely to occur, too proximal (in the compact bone of the diaphysis). The instances, where the position of the plate was questionable, particularly in the early phase of the experiments, were managed on the case-by-case basis. If, during the operation, the position of the plate looked suboptimal, I would attempt to reposition the plate, and most of the times I would achieve a better fixation. However, there were a few cases where I was not able to achieve a better plate position. Sometimes it was because I could not get the distal screw to engage with the bone, which becomes slanted at its distal end. However, a bigger challenge was to make small positional adjustments of already miniature-sized implant.

b) Close proximity of the growth plate: the growth plate lies within the metaphysis. Injuring the growth plate can lead to excessive new bone formation and thereby growth of the bone in this region, leading to bone deformities (mal-alignment). In distal femur of a mouse, epiphyseal growth plate is situated immediately distal to its metaphysis. The ideally positioned MouseFix® plate is centered over the metaphyseal osteotomy, and is fixed to the femur with two screws proximal to the osteotomy and one screw distal both to the osteotomy and the growth plate. Because of the miniature size of the plate, it is very easy to place the plate either too proximally or too distally to its ideal position. If the plate is placed too proximally, the distal screw can end up in the growth plate and lead to its injury. Similarly, a plate, which is too distal, may cause the osteotomy to be created in the growth plate instead of metaphysis, and lead to epiphyseal plate injury and/or growth plate arrest. Furthermore, this new callus tissue formed in addition to that which already formed as a part of normal healing. In such situations, the value of callus volume could be falsely elevated, because it is impossible to distinguish the old callus, formed after the original osteotomy, from the new callus, generated as a result of injury to the growth plate. Conversely, placement of the osteotomy in the diaphysis, and later including the area of bony defect in the calculation of the bone volume can result in falsely lower mean value, and, consequently, the lower mean value of the callus volume, masking the differences in callus volume between the groups.

c) The curved shape of the distal femur. The distal, metaphyseal aspect of the murine distal femur slants downwards and curves posteriorly as it approaches the knee joint. Positioning the straight fixation plate over this curved region of the bone therefore proved to be difficult. As per instructions, the plate is ideally placed with the central section of the plate (in the region where the osteotomy is to be placed)

closest to the bone, while the proximal and distal component of the plate stand off the bone at similar distances (Fig 33). However, if the plate is placed too distally, it will hang over the arched portion of the femoral condyle, with subsequent weaker contact of the plate with the bone in the proximal segment, which may lead to the screws pulling out of the bone.

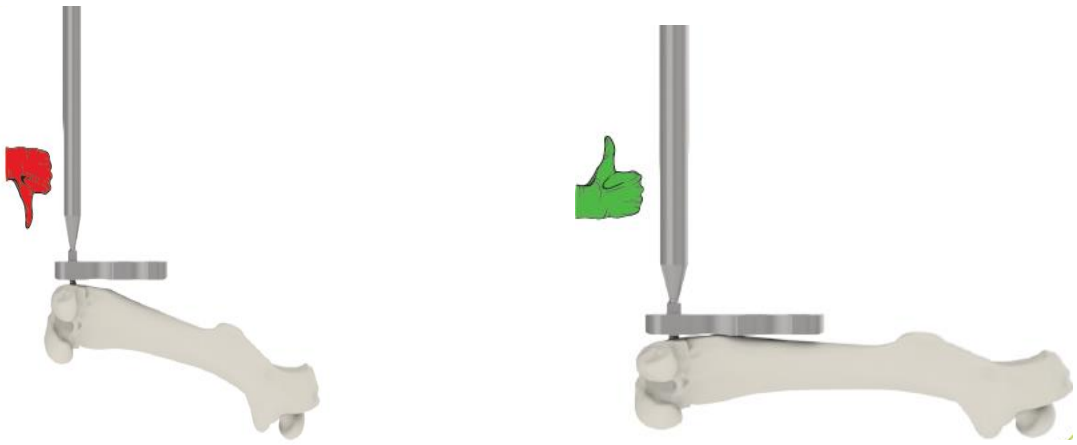

a) b)

Fig 33.a) incorrect position of the MouseFix® plate, with proximal part too far away from the femoral shaft a) correct position of the MouseFix® plate, with both ends equidistant from the femur (RISystem 2009)

Vice versa, if the plate is touching the bone at the proximal section, the distal portion of the plate stands off too far off the distal femur to ensure secure fixation to the bone. In contrast to the diaphyseal MouseFix® system, for the metaphyseal plates there is no drill guide available, which ordinarily allows precise screw position and osteotomy placement. Due to the curved shape of the distal femur, it was necessary to use a free-hand method of plate positioning and screw insertion, which could be another source of variability in plate and osteotomy positioning.

Histing et al (Histing, Klein et al. 2012) performed the same operation for their study, and they experienced similar difficulties. They attributed screw pullouts to a weaker trabecular bone structure in metaphyseal region rather than condylar curvature causing increased strain on the distal screws. This can usually be avoided

by placing the plate on the lateral aspect of the femur where the plate remains in the metaphyseal area, but is not hindered by the posterior sloping of the distal femur. However, the position of several plates, particularly in the early stages of the experiment, was either partially or completely in the diaphysis instead of the metaphysis. Unfortunately, we did not have postoperative x-ray control available during this study, therefore there was no immediate feedback after each surgery, and consequently the learning curve of the investigator performing surgeries was longer, which could account for the cases of suboptimal plate positioning at the beginning of the study.

As part of the normal postoperative monitoring, the mice were inspected daily by the investigators and experienced animal handlers. Any visible change in their mobility or the state of the wound was promptly recorded on monitoring sheets, and the mouse would then be watched more closely. In this study, only one animal was found limping on the operated leg, indicating pain was experienced by the animal, which was consequently sacrificed. The remaining animals showed no evidence of gait abnormality. After the sacrifice, the bones were again closely inspected, and if re-fracture or growth plate arrest was suggested (i.e by gross instability, massive callus or obvious mal-alignment), such specimens were excluded from further testing. It is quite possible that some of the tested specimens sustained a small re-fracture, or had a growth plate injury at some point during or after surgery, which re-invigorated the callus-forming process, but the change was not big enough to produce an abnormality, visible to a naked eye. Furthermore, if the plate was completely in diaphysis, then the specimen was excluded from the study. If, however, the plate was partially in metaphysis, its position was reassessed: if on

visual examination a larger portion was in the metaphysis, the specimen was kept, but if only a small part was in the metaphysis, the specimen was excluded.

Due to the limitations listed above, it was impossible to control the biomechanical conditions in this study sufficiently, mainly because of the difficulties with plate positioning. In addition, in excluding animals from the study, we had to balance the purpose of this study with the relatively small sample population. The variability of our results suggests a lack of standardization and reproducibility of the current method.

After these issues were identified during the mechanical testing and microCT evaluation of the study, we decided to limit the histologic evaluation to three animals with ideal implant position per experimental group and time point. This reduction in sample size represents a further limitation of the evaluation methods, which could have skewed the results. There were also unavoidable technical obstacles, associated with the challenges of histological evaluations of preclinical studies. Bone positioning during embedding is challenging, therefore it can be difficult to obtain consistently identical cuts from decalcified tissues. Due to the small number of samples available for histological evaluation, we only performed qualitative histological examinations by microscopic inspection of the histological sections. Larger sample sizes and formal quantitative histomorphometric analysis, such as by the point-counting method, would yield more information on exact amount of cartilage and other tissue types present in each group.

Furthermore, our method of mechanical testing carried all the risks, associated with the mechanical testing of small samples. While torsional testing is the method of choice for the evaluation of healing diaphyseal fractures, the extremely small distal component of the bones with a fracture in the metaphyseal

bone of the distal femur makes the fixation (through potting or other measures) of the distal component almost impossible. It was therefore decided to use an adapted 3-point bending system for the testing of the bones in our experiments, which eliminates the need for fixation of the distal fragment. However, as per bending theory, in order to produce accurate results, the length of the loaded specimen should be sufficiently long, compared to its cross section. Generally, the length-to-width ratio of the specimen should be at least 16:1, otherwise, excessive shear forces will be generated in the middle of the bone when the load is applied to shorter specimens (Turner 2006). This relationship was not possible to achieve in current experiment, we therefore acknowledge that primarily the shear strength of the healing bones was tested in our experiments.

In summary, our attempt to answer the original research question has been hampered by challenges, such as the small animal size and small study sample, combined with the extremely narrow safe margin of error in osteotomy placement and absence of intra- and post-operative x-ray control.

However, we hope that the difficulties we experienced will help researchers, contemplating using the MouseFix® implants in their future experiments. To improve the technical aspect of this study, we recommend the following measures:

a) design of a dedicated metaphyseal MouseFix® plate, curved at the distal end to conform to the slanting portion of the distal femur

b) use of intra-/ and postoperative x-rays to confirm placement of the implants in the correct region on the bone

c) completion of the learning curve by the operator prior to beginning of surgeries (cadaveric specimens are available in most institutions)

In the future experiments, it would also be beneficial to investigate the information contained in the microCT scans, for example, by comparing peak grayscale values between specimens before thresholding, as it may contribute valuable information regarding the degree of mineralisation of the callus. Finally, a more detailed characterisation of bending and torsional stiffness differences between the implants will be beneficial for interpretation of results.

Conclusions

The high variability of the results of this study, caused by limitations of the experimental model, has not allowed us to answer our original research questions successfully. Our histological results are observational findings from limited amount of histological data. Regardless of fixation stiffness, metaphyseal bones heal through a combination of intramembranous and endochondral ossification. Further attempts to determine the influence of fixation stiffness on callus size or mechanical integrity were inconclusive. We therefore suggest significant improvements to the experimental model, before further attempts to study metaphyseal bone fracture healing in mice are made.

REFERENCES

Aaron, J. (2012). "Periosteal Sharpey's fibers: a novel bone matrix regulatory system?" Front Endocrinol **3**: 98.

Abramoff, M., et al. (2004). "Image Processing with ImageJ." J Biophotonics **11**(7): 36-42.

Alffram, P.-A. and G. Bauer (1962). "Epidemiology of Fractures of the Forearm A Biomechanical Investigation of Bone Strength " The Journal of Bone & Joint Surgery **44**: 105-114.

Alffram, P.-A. and G. C. H. Bauer (1962). "Epidemiology of fractures of the forearm: a biomechanical investigation of bone strength " The Journal of Bone and Joint Surgery **44**: 105-114.

An, Y. and K. Martin (2003). Handbook of histology: methods for bone and cartilage, Humana Press.

Arnsdorf, E., et al. "The periosteum as a cellular source for functional tissue engineering." Tissue Eng **15**(9): 2637-2642.

Aronson, J. and X. Shen (1994). " Experimental healing of distraction osteogenesis comparing metaphyseal with diaphyseal sites." Clin Ortho Relat Rsch **301**: 25-30.

Bales, J. G. and P. J. Stern (2012). "Treatment strategies of distal radius fractures." Hand Clin **28**(2): 177-184.

Bell, A., et al. (2000). "Characteristics and outcomes of older patients presenting to the emergency department after a fall: a retrospective analysis." MJA **173**(4): 176-177.

Bird, J. and C. Ross (2012). Mechanical Engineering Principles, Routledge.

Bostrom, M. (1998). "Expression of bone morphogenetic proteins in fracture healing." Clin Orthop Relat Res **355**: S116-123.

Brookes, M. (1974). "Approaches to non-invasive blood flow measurement in bone." Biomed Eng. **9**(8): 342-347.

Claes, L., et al. (2009). "Hyperhomocysteinemia is associated with impaired fracture healing in mice" Calcif Tissue Int(85): 17-21.

Claes, L., et al. (2011). "Late dynamization by reduced fixation stiffness enhances fracture healing in a rat femoral osteotomy model." J Orthop Trauma **25**: 169-174.

Claes, L. and J. L. Cunningham (2009). "Monitoring the Mechanical Properties of Healing Bone." Clin Orthop Relat Res **467**: 1964-1971.

Claes, L., et al. (2011). "Metaphyseal fracture healing follows similar biomechanical rules as diaphyseal healing." Journal of Orthopaedic Research **29**(3): 425-432.

Claes, L. E. and J. L. Cunningham (2009). "Monitoring the mechanical properties of the healing bone." Clin Orth Rel Res **467**(8): 1964-1971.

Claes, L. E., et al. (1998). "Effects of mechanical factors on the fracture healing process." Clinical Orthopaedics And Related Research **355**(Supple): S132-S147.

Claes, L. E., et al. (1995). "Osteonal structure better predicts tensile strength of healing bone than volume fraction." Journal of Biomechanics **28**(11): 1377-1390.

Cook, R. and P. Zioupos (2009). "The fracture toughness of cancellous bone." J Biomech **42**(13): 2054-2060.

Cox, A., et al. (2009). "A New Standard Genetic Map for the Laboratory Mouse " Genetics **182**: 1335-1344.

Cruess, R. and J. Dumont (1975). Healing of bone, tendon and ligament. Philadelphia, JB Lippincott.

Cruess, R. and J. Dumont (1975). Healing of bone, tendon andligament. Philadelphia, JB Lippincott.

Cruess, R. L. and J. Dumont (1975). "Fracture healing." Canadian journal of surgery. Journal canadien de chirurgie **18**(5): 403-413.

Davies, J. (2001). "The rising number of underfoot accidents after the menopause causes both fracture and non-fracture injuries." J Med **94**: 699-707.

Diaz-Garcia, R., et al. (2011). "A systematic review of outcomes and complications of treating unstable distal radius fractures in the elderly." J Hand Surg Am **36**(5): 824-835.

Dimitriou, R., et al. (2005). "Current concepts of molecular aspects of bone healing." Int J care injured **36**: 1392-1404.

Drobetz, H., et al. (2006). "Volar fixed-angle plating of distal radius extension fractures: influence of plate position on secondary loss of reduction--a biomechanic study in a cadaveric model." J Hand Surg Am **31**(4): 615-622.

Dwek, J. (2010). "The periosteum: what it is, where is it, and what mimics it in its absence?" Skeletal Radiol **39**(4): 319-323.

Earnshaw, S. A., et al. (1998). "Colles' Fracture of the Wrist as an Indicator of Underlying Osteoporosis in Postmenopausal Women: A Prospective Study of Bone Mineral Density and Bone Turnover Rate." Osteoporosis International **8**(1): 53-60.

Egermann, M., et al. (2010). "Influence of defective bone marrow osteogenesis on fracture repair in an experimental model of senile osteoporosis." Journal of Orthopaedic Research **28**(6): 798-804.

Egol, K., et al. (2010). "Distal radial fractures in the elderly: operative compared with nonoperative treatment." JBJS (Am) **92**(9): 1851-1857.

Einhorn, T. (1998). "The cell and molecular biology of fracture healing." Clinical orthopedics and related research **355**: S7-S21.

Einhorn, T. (2005). "The science of fracture healing." Journal of orthopedic trauma **19**: S4-S6.

Epari, D. (2006). The mechanobiology of diaphyseal secondary bone healing. Engineering. Berlin, der Technischen Universität Berlin. **PhD**.

Epari, D. R., et al. (2006). "Instability prolongs the chondral phase during bone healing in sheep." Bone **38**(6): 864-870.

Fan, W., et al. (2010). "Structural and cellular features in metaphyseal and diaphyseal periosteum of osteoporotic rats." J Mol Histol **41**(1): 51-60.

Frost, H. (1989). "The biology of fracture healing: an overview for clinicians. Part I." Clin Orthop Relat R **248**: 283-293.

Goldhaber, P. (1961). "Osteogenic induction across millipore filters in vivo." Science **133**(3470): 2065-2067.

Goulding, A., et al. (2001). "Bone mineral density and body composition in boys with distal forearm fractures: a dual-energy x-ray absorptiometry study." J Pediatr **39**(4): 509-515.

Greene, W. (2005). Netter's Orthopaedics. New York, Elsevier Inc. .

Gröngröft, I., et al. (2009). "Fixation compliance in a mouse osteotomy model induces two different processes of bone healing but does not lead to delayed union." J Biomech **42**(13): 2089-2096.

Gröngröft, I., et al. (2009). "Fixation compliance in a mouse osteotomy model induces two different processes of bone healing but does not lead to delayed union." Journal of Biomechanics **42**(13): 2089-2096.

Hall, B. and H. Jacobson (1975). " The repair of fractured membrane bones in the newly hatched chick." Anat Rec **181**: 55-69.

Han, N., et al. (2012). "A new experimental model to study healing process of metaphyseal fracture." Chin Med J (Engl) **125**(4): 676-679.

Hausdorff, J., et al. (2001). "Gait variability and fall risk in community–living older adults: a 1–year prospective study." Arch Phys Med Rehabil **82**(8): 1050-1056.

Helgason, H. (2008). "Mathemathical relationships between bone density and mechanical properties." Clinical Biomechanics **23**(2): 135-146.

Hente, R., et al. (2003). "In vivo measurement of bending stiffness in fracture healing." Biomed Eng Online **2**: 8.

Histing, T. (2009). "Ex vivo analysis of rotational stiffness of different osteosynthesis techniques in mouse femur fracture." Journal of Orthopaedic Research.

Histing, T., et al. (2011). "Small animal bone healing models: Standards, tips, and pitfalls results of a consensus meeting." Bone **49**: 591-599.

Histing, T., et al. (2012). "A new model to analyze metaphyseal bone healing in mice." J Surg Res **178**(2): 715-721.

Holstein, J., et al. (2009). "Development of a stable closed femoral fracture model in mice." J Sur Res **153**: 71-75.

Hutmacher, D. and M. T. E. S. S.-. Sittinger (2003). "Periosteal cells in bone tissue engineering." Tissue Eng **9** (Suppl 1): S45-64.

Jager, T., et al. (2000). "Traumatic brain injuries evaluated in U.S. emergency departments, 1992–1994." Acad Emerg Med **7**(2): 134-140.

Jarry, L. and H. Uhthoff (1971). "Differences in healing of metaphyseal and diaphyseal fractures. ." Can J Surg **14**: 127–135.

Jupiter, J. and M. Marent-Huber (2010). "Operative management of distal radial fractures with 2.4-millimeter locking plates: a multicenter prospective case series. Surgical technique." JBJS (Am) **92 (Suppl)**: S96-106.

Kemp, A., et al. (2008). "Patterns of skeletal fractures in child abuse: systematic review." BMJ **337**(7674).

Khosla, S., et al. (2003). "Incidence of childhood distal forearm fractures over 30 years: a population-based study." JAMA **290**(11): 1479-1485.

Kleinman, P. (1998). Diagnostic Imaging of Child Abuse.

Knox, J., et al. (2007). "Percutaneous pins versus volar plates for unstable distal radius fractures: a biomechanic study using a cadaver model." J Hand Surg Am **32**(6): 813-817.

Koenig, K., et al. (2009). "Is early internal fixation preferred to cast treatment for well-reduced unstable distal radial fractures?" JBJS (Am) **91**(9): 2086-2093.

Kopeliovich, D. (2012). Substances and Technologies.

Marks, S. and D. Hermey (1996). The structure and development of bone. Principles of bone biology. J. Bilezikan, L. G. LG Raisz and G. Rodan. San Diego, Academic Press. **I:** 3-14.

Marsell, R. and T. Einhorn (2011). "The biology of fracture healing." Injury **42**(6): 551-555.

Martin, B., et al. (1998). Skeletal Tissue Mechanics, Springer.

Martin, R. and D. Burr (1989). Structure, function, and adaptation of compact bone. New York, Raven Press.

Martini, L., et al. (2001). "Sheep model in orthopedic research: a literature review " Comparative Med **51**(4): 292-299.

Marzona, L. and B. Pavolini (2009). "Play and players in bone fracture healing match." Clinical cases in mineral and bone metabolism : the official journal of the Italian Society of Osteoporosis, Mineral Metabolism, and Skeletal Diseases **6**(2): 159-162.

Matthys, R. and S. M. Perren (2009). "Internal fixator for use in the mouse." Injury **40, Supplement 4**(0): S103-S109.

McKibbin, B. (1978). "The biology of fracture healing in long bones." The Journal of Bone and Joint Surgery **60B**: 150-162.

Mercurio, A., et al. (2012). "Effects of extensive periosteal stripping on the microstructure and mechanical properties of the murine femoral cortex." J Orthop Res **30**(4): 561-568.

Merloz, P. (2011). "Macroscopic and microscopic process of long bone fracture healing." Osteoporos Int **22**(6): 1999-2001.

Miller, S., et al. (1985). "Fractures of the distal forearm in Newcastle: an epidemiological survey." Age Ageing **14**(3): 155-161.

Minnesota, U. o. (2009). "Research Animal Guidelines." Euthanasia guidelines. Retrieved June 5, 2013, from http://www.ahc.umn.edu/rar/euthanasia.html.

Morris, M. and P. Kelly (1980). "Use of tracer microspheres to measure bone blood flow in conscious dogs." Calcif Tissue Int **32**(1): 69-76.

Nana, A., et al. (2005). "Plating of the distal radius." J Am Acad Orthop Surg **13**(3): 159-171.

Newton, C. and D. Nunamaker (1985). Healing of bone. Textbook of small animal orthopaedics. C. Newton, J.B.Lippincott Co.

National Health and Medical Research Council (NHMRC) (2008). "Guidelines to promote the wellbeing of animals used for scientific purposes: The assessment and alleviation of pain and distress in research animals.". Retrieved Nov 2, 2013, from http://www.nhmrc.gov.au/guidelines/publications/ea18.

Nuss, K., et al. (2006). "An animal model in sheep for biocompatibility testing of biomaterials in cancellous bones." BMC Musculoskelet Disord(7): 67.

Oh, C., et al. (2003). "Distal tibia metaphyseal fractures treated by percutaneous plate osteosynthesis." Clin Orthop **408**: 286-291.

Orbay, J. and D. Fernandez (2004). "Volar fixed-angle plate fixation for unstable distal radius fractures in the elderly patient." The Journal of Hand Surgery **29A**(1): 96-102.

Periosteum, I. a. M. C. o. t. H., et al. (2013). "Immunohistochemical and molecular characterization of the human periosteum." Sci World J.

Perren, S. (1979). "Physical and biological aspects of fracture healing with special reference to internal fixation." Clin Orthop Relat R **138**: 175-196.

Perren, S. and J. Cordey (1980). The concept of interfragmentary strain. Current Concepts of Internal Fixation of Fractures. H. Unthoff. Berlin, Springer.

Rauch, F., et al. (2001). "The development of metaphyseal cortex--implications for distal radius fractures during growth." J Bone Miner Res **16**(8): 1547-1555.

Rauch, F., et al. (2001). "The development of metaphyseal cortex -- implications for distal radius fractures during growth." Journal of Bone and Mineral Research **16**(8): 1547-1555.

RISystem (2009). "Standardized Systems for Use in Research." MouseFix. Retrieved Sep 23, 2013.

RISystem (2009). "Standardized Systems for Use in Research." MouseFix. Retrieved Sep 23, 2013, from http://www.risystem.com/Standardized_Implant_for_Research/RISystem.html.

Robinson, C., et al. (2003). "Adult distal humeral metaphyseal fractures: epidemiology and results of treatment." J Orthop Trauma **17**(1): 38-47.

Rüedi, T., et al. (2007). AO Principles of Fracture Management, Thieme.

Schell, H., et al. (2005). "The course of bone healing is influenced by the initial shear fixation stability." J Orthop Res **23**(5): 1022-1028.

Schmidt-Bleek, K., et al. (2012). "Inflammatory phase of bone healing initiates the regenerative healing cascade." Cell and Tissue Research **347**(3): 567-573.

Shefelbine, S. and e. al (2005). "Intact fibula improves fracture healing in a rat tibia osteotomy model." Journal of Orthopaedic Research **23**: 489-493.

Shefelbine, S. J., et al. (2005). "Trabecular bone fracture healing simulation with finite element analysis and fuzzy logic." Journal of Biomechanics **38**(12): 2440-2450.

Smith, D. and M. Henry (2005). "Volar fixed-angle plating of the distal radius." J Am Acad Orthop Surg **13**(1): 28-36.

Steck, R., et al. (2011). "Influence of internal fixator flexibility on murine fracture healing as characterized by mechanical testing and microCT imaging." J Orth Res **29**(8): 1245-1250.

Steck, R., et al. (2011). "Influence of internal fixator flexibility on murine fracture healing as characterized by mechanical testing and microCT imaging." J Orthopaed Res **29**(8): 1245-1250.

Thompson, Z., et al. (2002). "A model for intramembranous ossification during fracture healing." Journal of Orthopaedic Research **20**(5): 1091-1098.

Toms, A., et al. (2004). "Percutaneous plating of the distal tibia." J Foot Ankle Surg **43**: 199-203.

Tondevold, E. and P. Eliasen (1982). "Regional vascular volumes and dynamic haematocrit compared to regional perfusion in canine cancellous and cortical bone." Acta Orthop Scand**53**(2): 197-203.

Turner, C. (2006). "Bone strength: current concepts." Ann N Y Acad Sci **1068**: 429-446.

Turner, R. T., et al. (2001). "Animal models for osteoporosis." Rev Endocr Metab Disord **2**(1): 117-127.

Uhthoff, H. and B. Rahn (1981). "Healing patterns of metaphyseal fractures." Clin Orthop **160**: 295–303.

Utvåg, S., et al. (1996). "Effects of periosteal stripping on healing of segmental fractures in rats." J Orthop Trauma **10**(4): 279-284.

Uusitalo, H., et al. (2001). "A metaphyseal defect model of the femur for studies of murine bone healing." Bone **28**(4): 423-429.

Uzwiak, T. (2013). Anatomy and Physiology: Bone I.

van Aaken, J., et al. (2009). "Long-term outcomes of closed reduction and percutaneous pinning for the treatment of distal radius fractures." J Hand Surg-Am **34**(5): 963.

Wang, Q., et al. (2010). "Rapid growth produces transient cortical weakness: a risk factor for metaphyseal fractures during puberty." J Bone Miner Res **25**(7): 1521-1526.

Weinera, S., et al. (1999). "Lamellar bone: structure-function relations." *Journal of Structural Biology **126**(3): 241-255.

WJ, K. (1968). "Fundamental concepts in bone-blood flow studies." J Bone Joint Surg Am. **50**(4): 801-811.

Yang, S.-W., et al. (2006). "Treatment of distal tibial metaphyseal fractures: plating versus shortened intramedullary nailing." Injury **37**(6): 531-535.

Yang, S., et al. (2006). "Treatment of distal tibial metaphyseal fractures: Plating versus shortened intramedullary nailing." Injury(37): 6.

Yingling, V. (2008). Structure of cancellous and cortical bone.

Young, B. and G. Rayan (2000). "Outcome following nonoperative treatment of displaced distal radius fractures in low-demand patients older than 60 years." J Hand Surg Am **25**(1): 19-28.

10. APPENDICES

APPENDIX I: Mechanical testing and microCT results

%Extrinsic Stiffness (%EI), N/mm, at 14 day time point

Mouse #	100% stiff (n = 7)	65% stiff (n = 7)	45% stiff (n = 9)
1	3.0	1.3	13.1
2	23.0	10.1	12.90
3	33.7	7.9	28.6
4	81.9	51.5	37.4
5	0.90	29.0	9.8
6	29.8	9.7	13.6
7	6.0	17.3	59.7
8			53.5
9			48.8
	Mean = 25.5+/-10.6	**Mean = 18.2+/-5.4**	**Mean = 30.6+/-6.5**

%Extrinsic Stiffness (%EI), N/mm, at 28 day time point

Mouse #	100% stiff (n = 7)	65% stiff (n = 5)	45% stiff (n = 9)
1	39.00	69.60	9.90
2	40.46	111.74	8.72
3	13.64	57.64	156.32
4	24.86	76.99	103.71
5	54.53	64.47	46.24
6	66.37		35.08
7	80.01		68.86
8			69.73
9			47.29
	Mean = 45.6 +/- 8.8	**Mean = 76.1 +/- 9.5**	**Mean = 60.7 +/-15.6**

Callus Volume (V_{call}), mm^3,at 14-day time point

Mouse #	100% stiff (n = 7)	65% stiff (n = 5)	45% stiff (n = 9)
1	767.0	772.0	795.0
2	816.0	760.4	731.0
3	766.5	760.6	767.1
4	773.1	787.6	772.7
5	744.4	869.4	774.1
6	755.0		774.2
7	781.9		765.9
8			755.1
9			792.8
	Mean = 772.0 +/- 8.4	**Mean = 769.8 +/- 6.5**	**Mean = 774.9 +/- 17.8**

Callus Volume (V_{call}), mm^3,at28-day time point

Mouse #	100% stiff (n = 7)	65% stiff (n = 5)	45% stiff (n = 9)
1	818.7	816.2	819.4
2	826.0	801.2	773.7
3	818.2	855.5	788.7
4	799.8	819.2	880.6
5	798.0	783.5	810.3
6	805.2		840.0
7	789.8		781.9
8			777.6
9			715.8
	Mean = 808.9 +/- 13.1	**Mean = 815.2 +/- 15.4**	**Mean = 789.7 +/- 11.3**

APPENDIX II: Histology slides

Haematoxylin and Eosin, H&E, stain

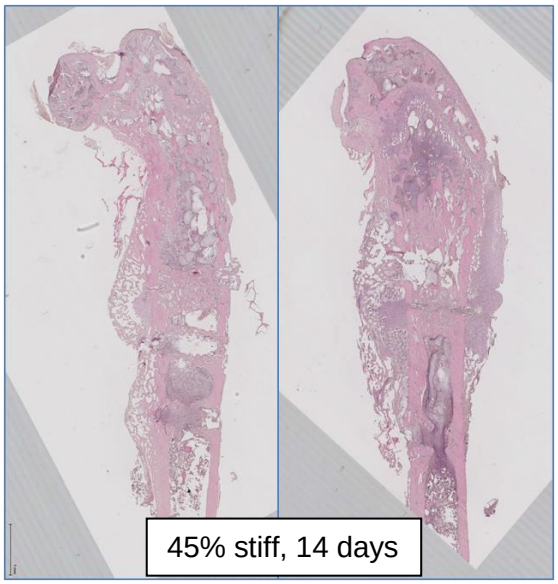

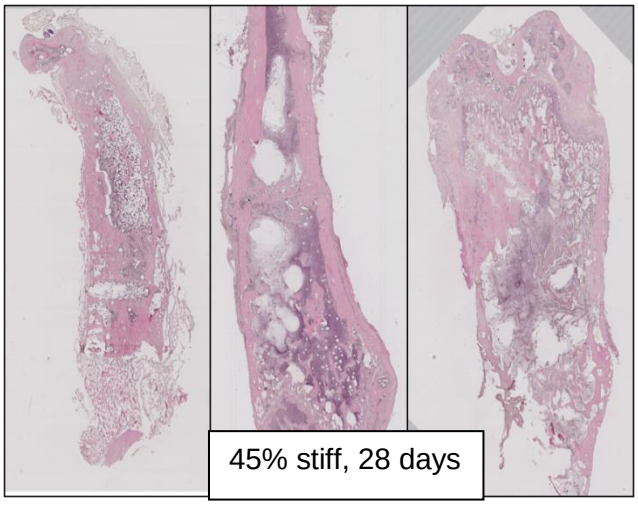

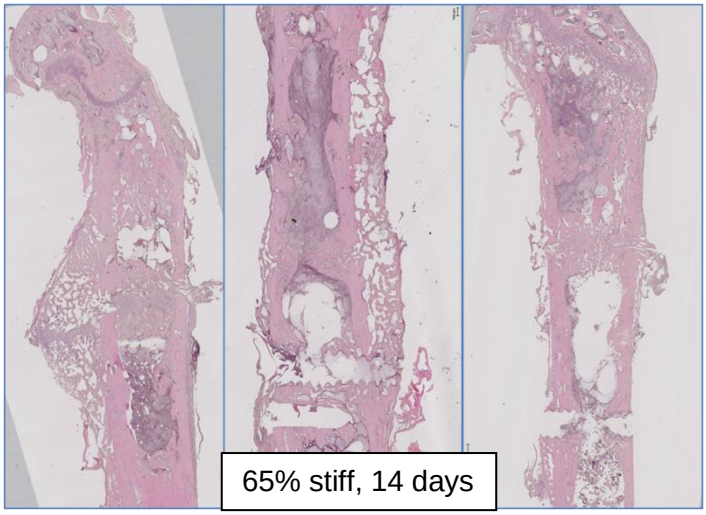

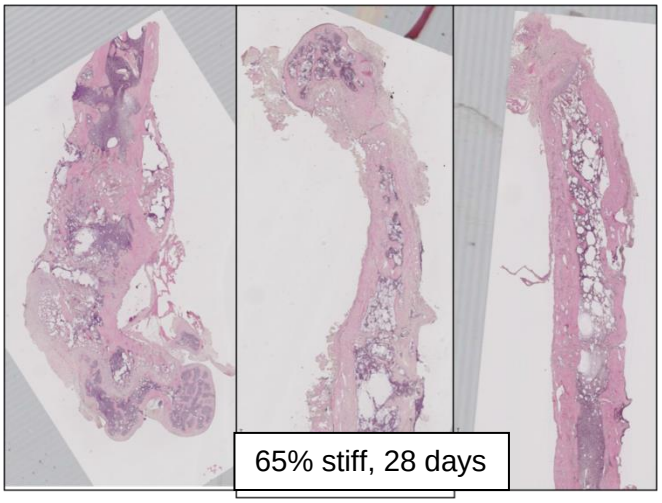

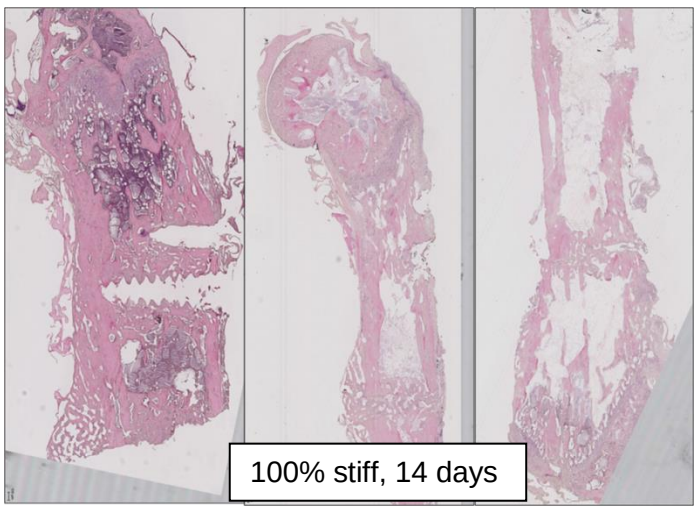

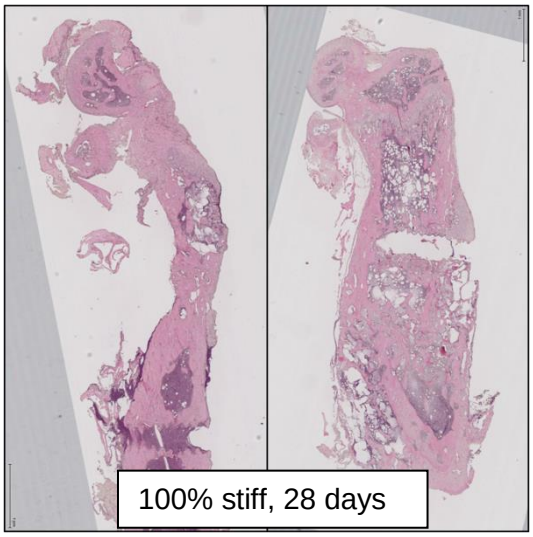

Safranin Orange, SafO, stain

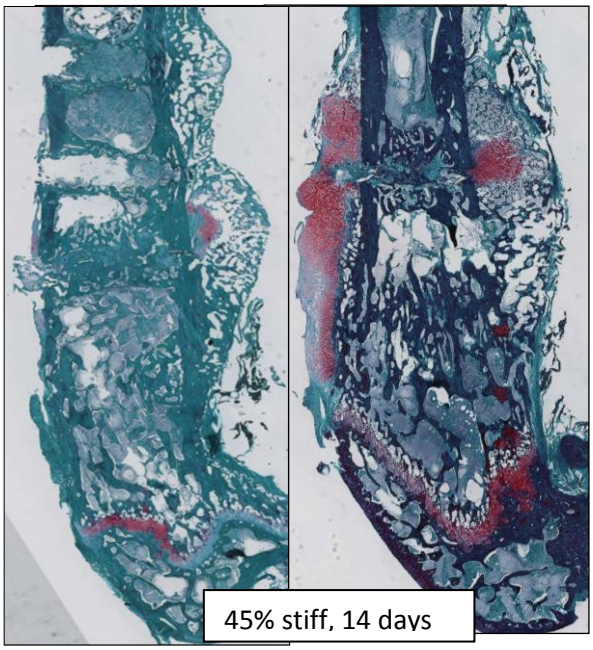

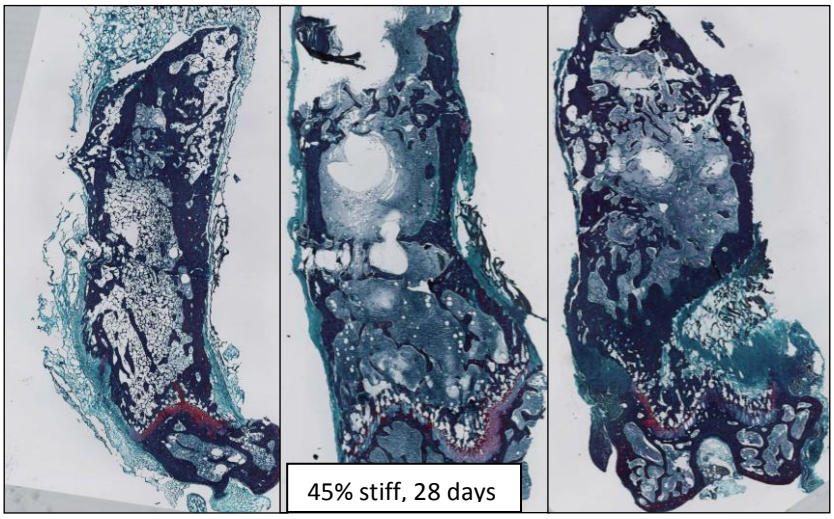

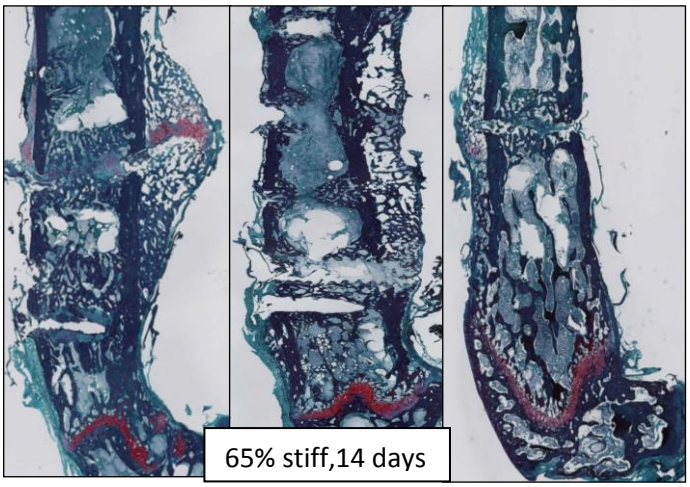

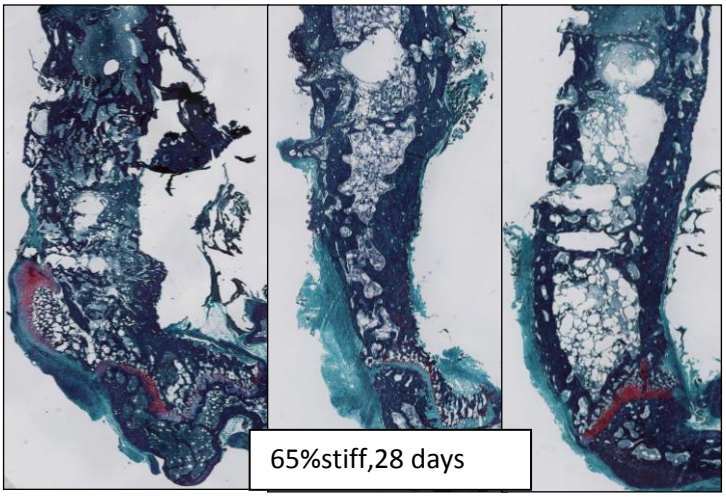

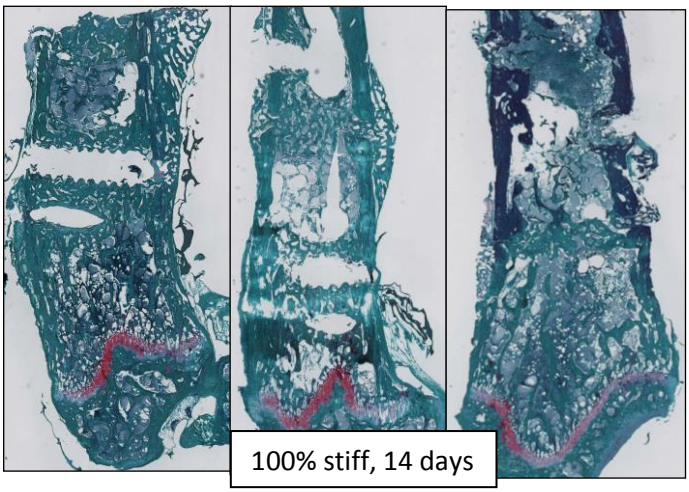

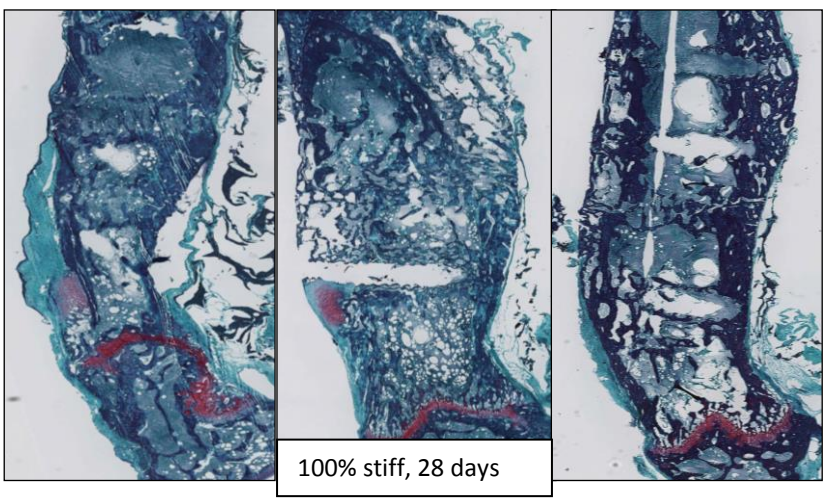

Appendix III: Mouse monitoring sheet

MOUSE MONITORING SHEET							
Mouse Details			First Noted (date)				
Phenotype			Exam Interval			Daily	
	Date						
UNDISTURBED							
Coat							
Activity							
Breathing							
Movement							
Eating							
Drinking							
WHEN HANDLED							
Activity							
Breathing							
Condition							
Surgery Site/Wound							
Comments							
INITIALS							

Appendix IV: Operation record template

QUT ihbi Institute of Health and Biomedical Innovation

MouseFix metaphyseal fracture healing

OPERATION – PROTOCOL – Osteotomy, MouseFix plate - Species: mouse (CD1, female)

Date: _ _ _ _ _ _ _ _

Animal No.:	Identification mark:

Age:	Weight:

Group:	**20% Flexible** fixation	**60% Flexible** fixation	**Rigid** fixation		
Keeping Time:			14 days	28 days	

1st surgeon:	2nd surgeon:	

Anaesthesia-Start:	Anaesthesia-Ending:
Surgery-Start:	Surgery-Ending:
Temgesic, s.c.:_____µl NaCl-Solution, s.c. : 0.5ml	
Comments:	

Signature _____ 1st surgeon _____ 2nd surgeon